The Electron-Ion Collider

Additional Material

Thomas Ullrich (BNL/Yale)
NNPSS, June 25/26, 2018

Yale BROOKHAVEN NATIONAL LABORATORY

Content (Additional Material)

A. Example of key measurements
   1. Spin of the proton
   2. Imaging
   3. Structure Functions and Nuclear PDFs in eA Collisions
   4. Dihadron Correlations
   5. Diffractive physics in eA

8. Few Examples of Key Measurements at an EIC

8.1 Spin of the Proton

EIC: Longitudinal Spin of the Proton (I)

Determine the contribution of quarks and gluons to the proton spin need to measure spin-dependent structure function g_1 as function of x and Q^2:

Inclusive Measurement:
$e+p \rightarrow e'+X$

$$\frac{1}{2}\left[\frac{\mathrm{d}^2\sigma^{\leftrightarrows}}{\mathrm{d}x\,\mathrm{d}Q^2} - \frac{\mathrm{d}^2\sigma^{\rightrightarrows}}{\mathrm{d}x\,\mathrm{d}Q^2}\right] \simeq \frac{4\pi\,\alpha^2}{Q^4} y\,(2-y)\,g_1(x,Q^2)$$

Leading Order: $$g_1(x,Q^2) = \frac{1}{2}\sum e_q^2\,\left[\Delta q(x,Q^2) + \Delta\bar{q}(x,Q^2)\right]$$

$$\Delta\Sigma(Q^2) = \int_0^1 dx\;g_1(x,Q^2)$$ (Quark Spin)

Higher Order: $$\frac{dg_1}{d\log Q^2} \propto \Delta g(x,Q^2)$$ (Gluon Spin)

EIC: Longitudinal Spin of the Proton (II)

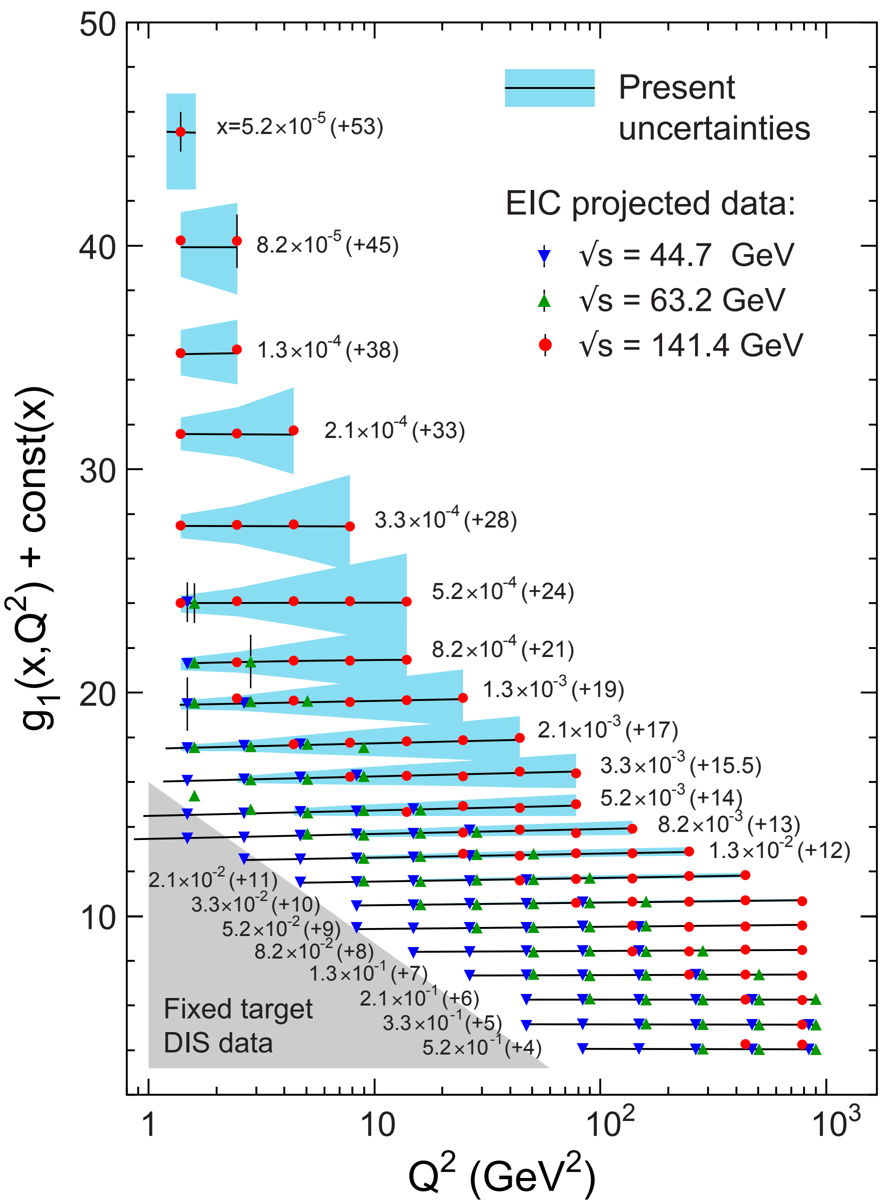

For $\int L dt$ = 10 fb^{-1} and 70% polarization

Current knowledge (DSSV): uses strong theoretical constraints

EIC projections do not $\Rightarrow$ test w/o assumptions

Recall Jaffe-Manohar sum rule:

$$\frac{1}{2} = \frac{1}{2}\int_0^1 \mathrm{d}x\Delta\Sigma(x,Q^2) + \int_0^1 \mathrm{d}x\Delta g(x,Q^2) + \sum_q L_q + L_g$$

Don't know what x contribute!
Need to measure over wide range down to lowest x.

EIC: Longitudinal Spin of the Proton (III)

Using the simulated $g_1(x,Q2)$ pseudo-data the following constrains on quark and gluon spin emerge:

EIC: Longitudinal Spin of the Proton (III)

Using the simulated $g_1(x,Q2)$ pseudo-data the following constrains on quark and gluon spin emerge:

Quark Spin

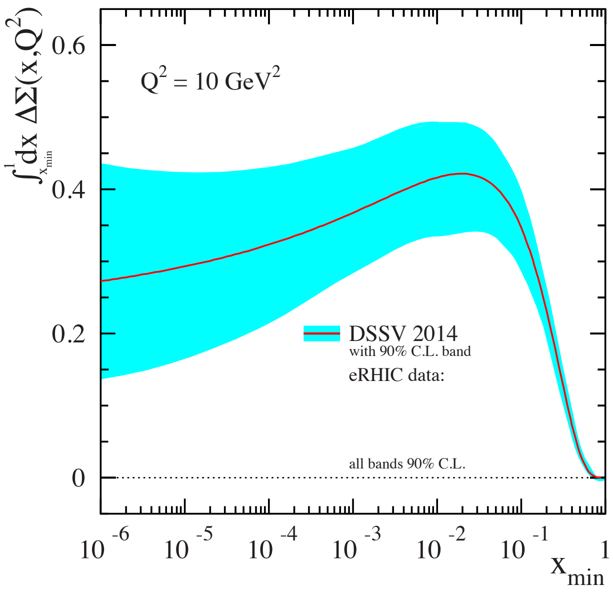

EIC: Longitudinal Spin of the Proton (III)

Using the simulated $g_1(x,Q2)$ pseudo-data the following constrains on quark and gluon spin emerge:

Quark Spin

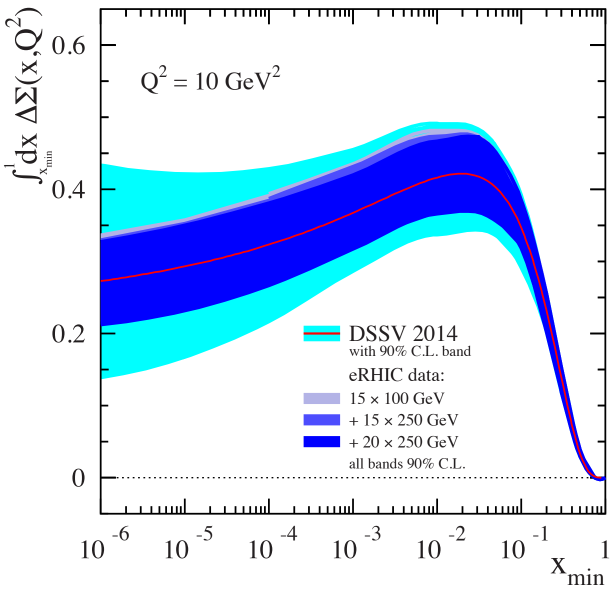

EIC: Longitudinal Spin of the Proton (III)

Using the simulated $g_1(x,Q2)$ pseudo-data the following constrains on quark and gluon spin emerge:

Quark Spin

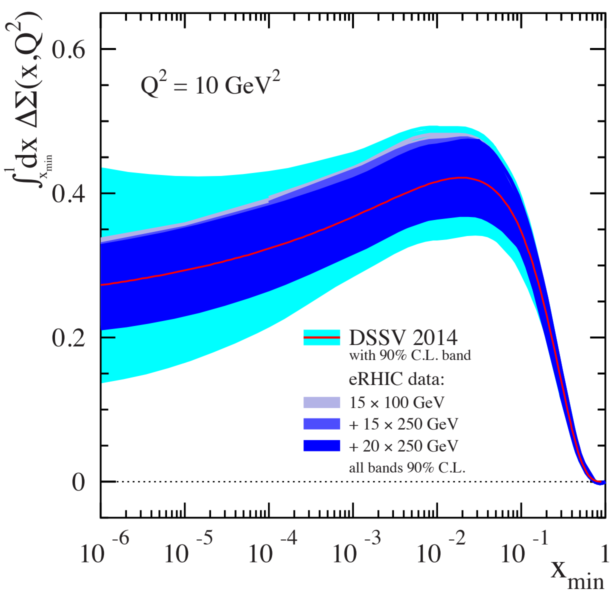

Gluon Spin

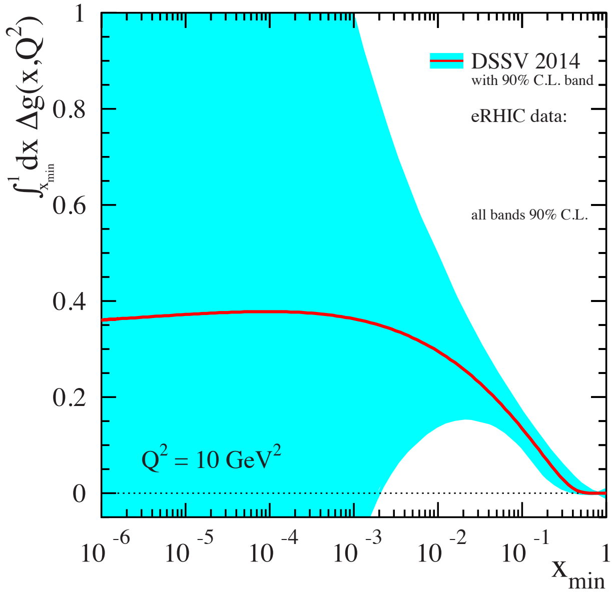

EIC: Longitudinal Spin of the Proton (III)

Using the simulated $g_1(x,Q2)$ pseudo-data the following constrains on quark and gluon spin emerge:

Quark Spin

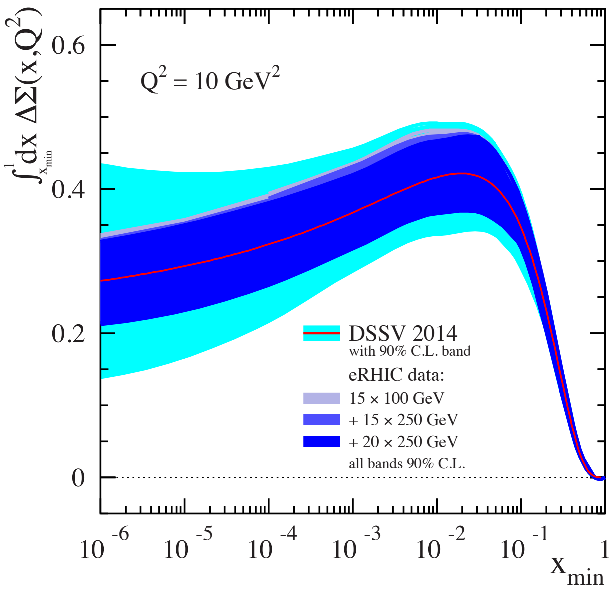

Gluon Spin

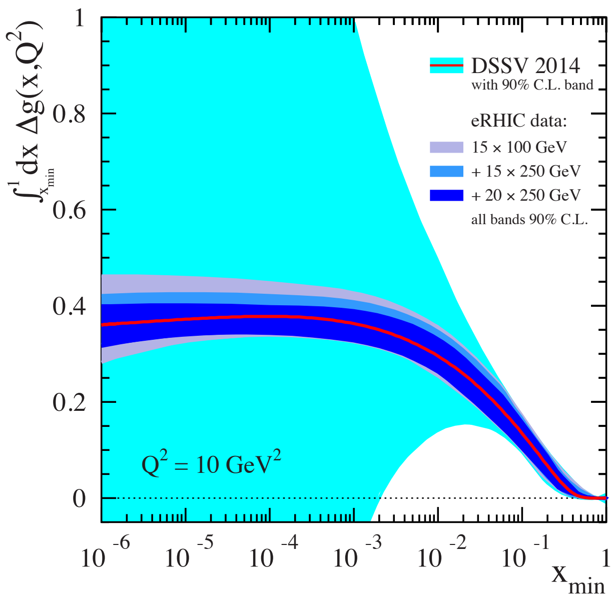

EIC: Longitudinal Spin of the Proton (III)

Using the simulated $g_1(x,Q2)$ pseudo-data the following constrains on quark and gluon spin emerge:

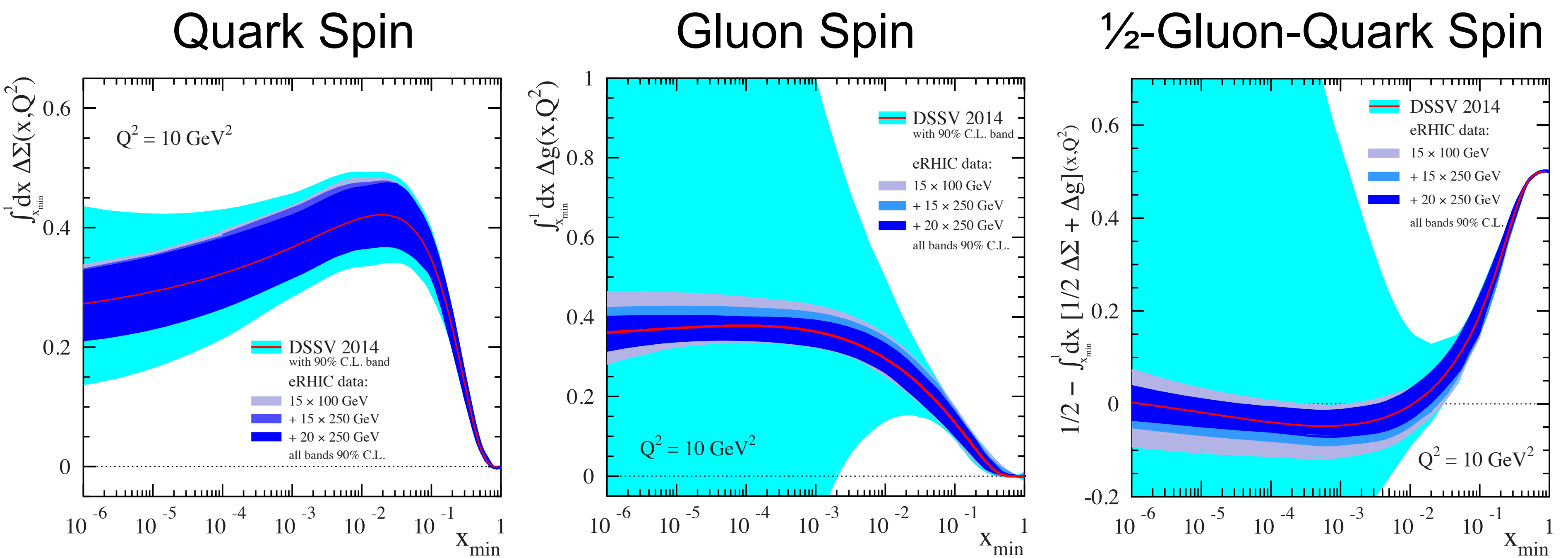

EIC: Longitudinal Spin of the Proton (III)

Using the simulated $g_1(x,Q2)$ pseudo-data the following constrains on quark and gluon spin emerge:

Combining information on $\Delta\Sigma$ and Δg constrains angular momentum

½-Gluon-Quark Spin

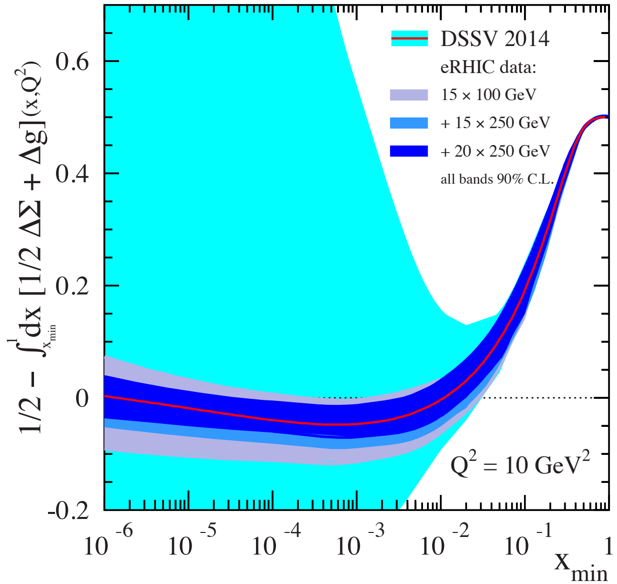

EIC: Longitudinal Spin of the Proton (IV)

Constraining spin of the sea-quarks and gluons at low-x is important but requires high √s

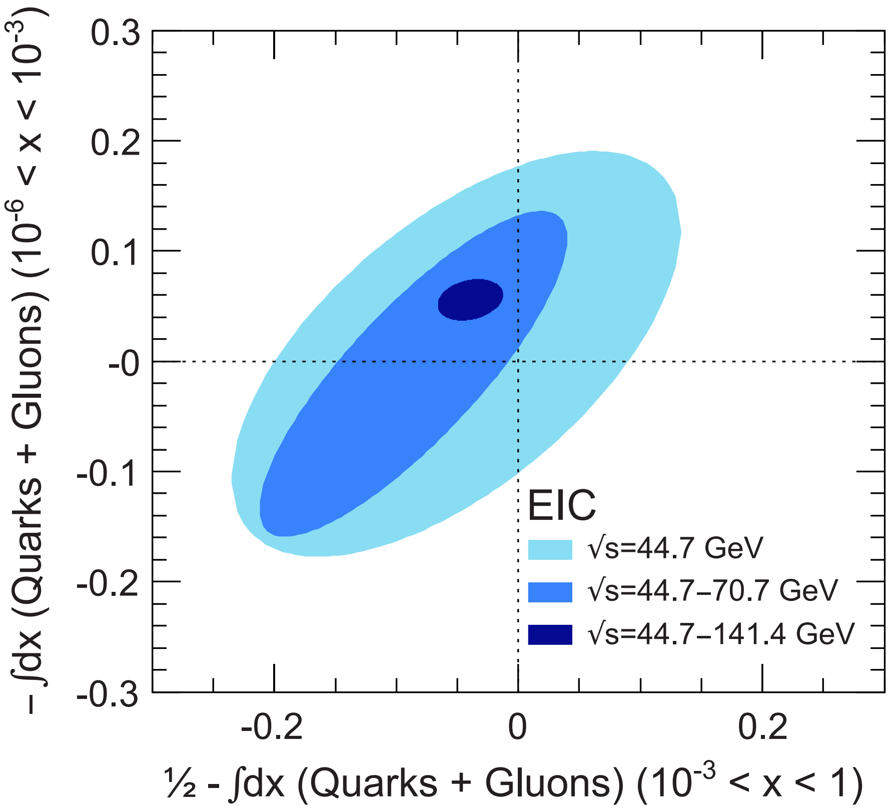

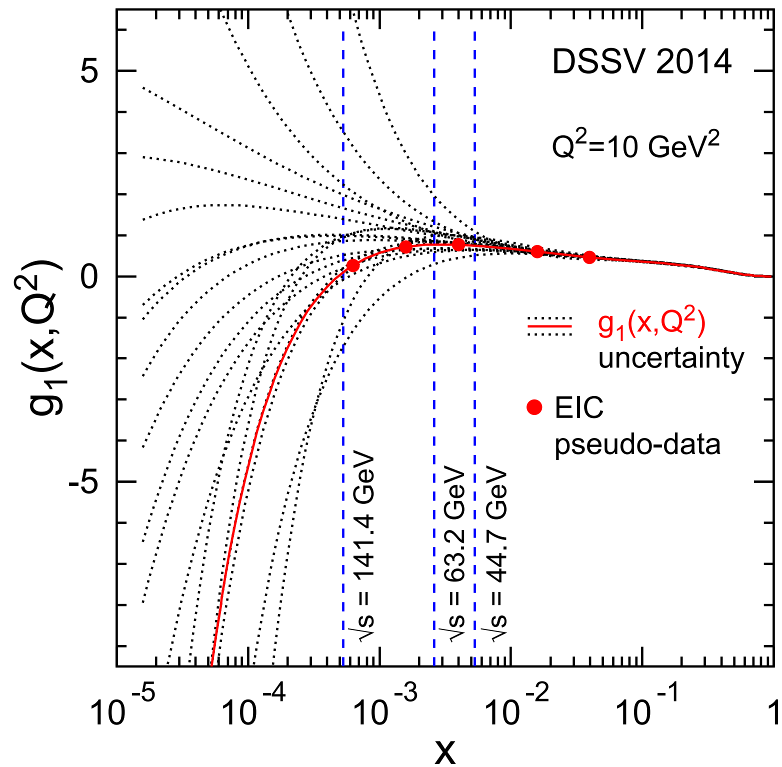

8.2 Imaging

3-D Imaging of Quarks and Gluons

$W(x,b_T,k_T)$

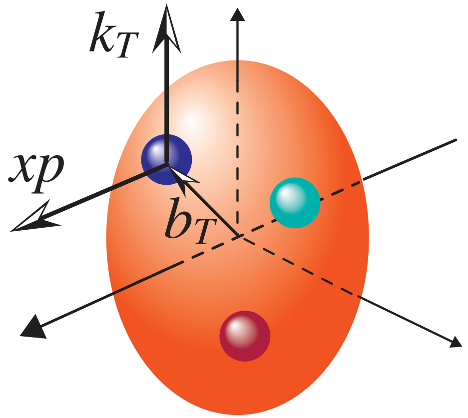

Mother of all functions describing the structure of the proton:

5D Wigner Function: $W(x, k_T, b_T)$

Was considered not measurable.
Recent ideas via dijet measurements are evolving …

3-D Imaging of Quarks and Gluons

$W(x,b_T,k_T)$

Momentum space

$\int d^2b_T$

$f(x,k_T)$

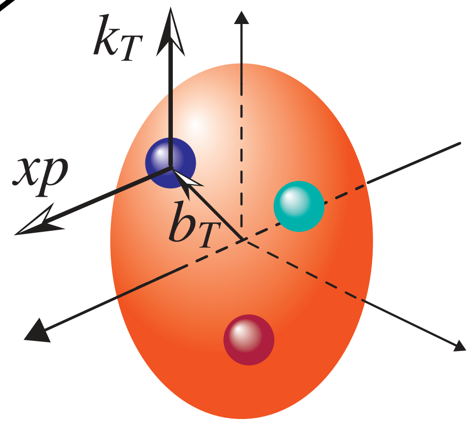

3-D Imaging of Quarks and Gluons

$W(x, b_T, k_T)$

Momentum space

$\int d^2 b_T$

$f(x, k_T)$

Quarks

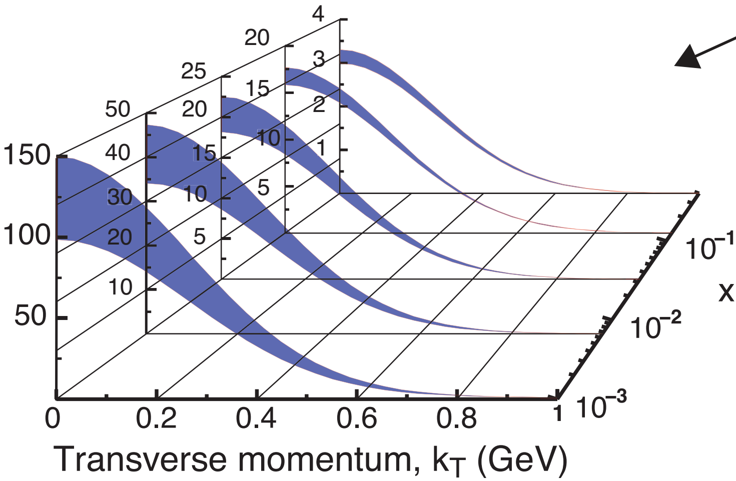

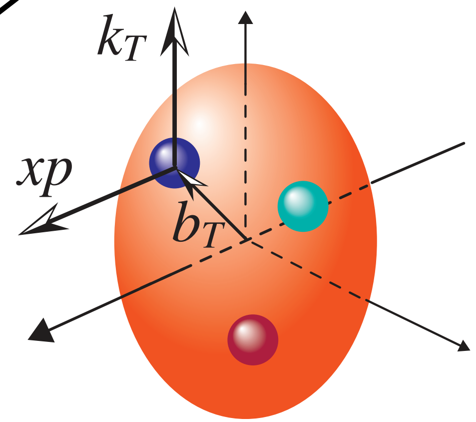

Spin-dependent 3D momentum space images from semi-inclusive scattering

Transverse Momentum Distributions (TMDs)

3-D Imaging of Quarks and Gluons

$W(x,b_T,k_T)$

Momentum space

$\int d^2b_T$

$\int d^2k_T$

Coordinate space

$f(x,k_T)$

$f(x,b_T)$

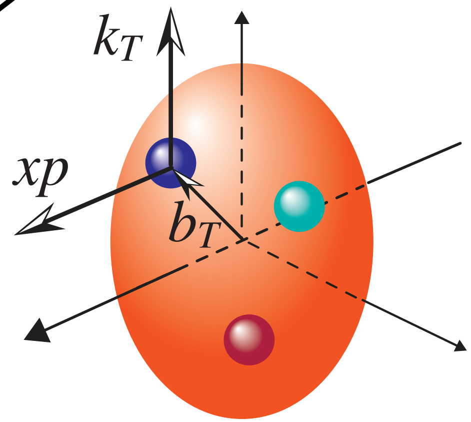

Quarks

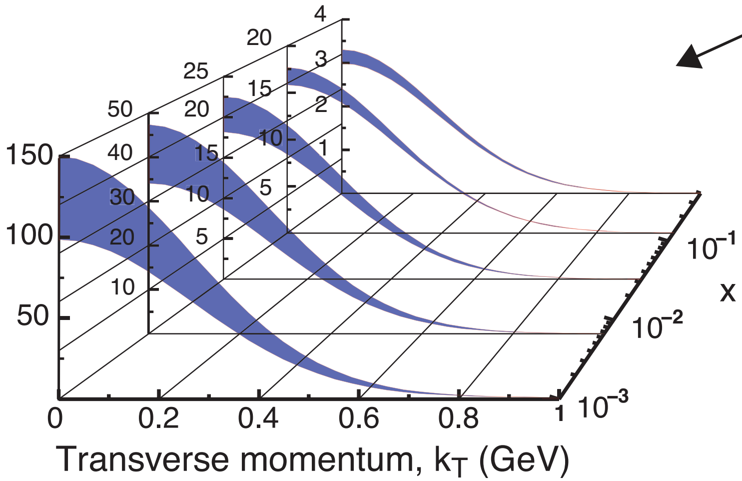

Spin-dependent 3D momentum space images from semi-inclusive scattering

Transverse Momentum Distributions (TMDs)

3-D Imaging of Quarks and Gluons

Momentum space

Coordinate space

$W(x,b_T,k_T)$

$\int d^2b_T$ $\int d^2k_T$

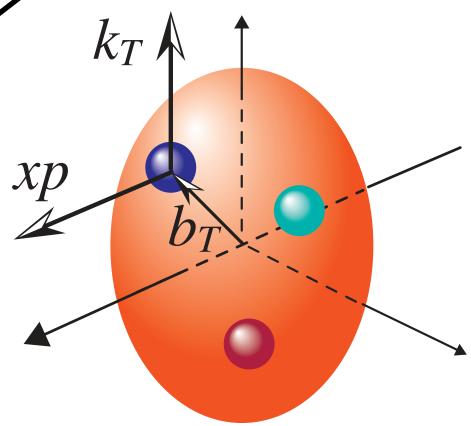

Quarks $f(x,k_T)$

$f(x,b_T)$ Gluons

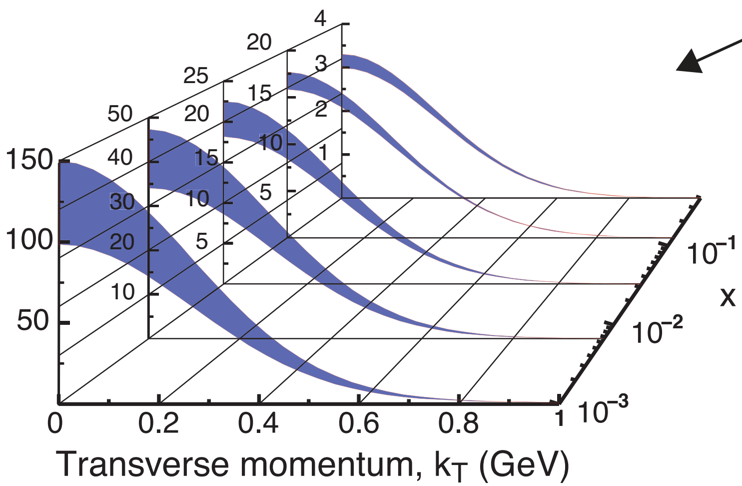

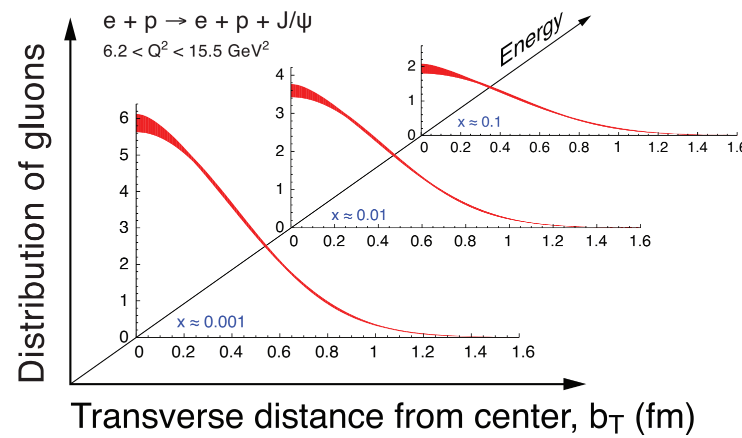

Spin-dependent 3D momentum space images from semi-inclusive scattering

Spin-dependent 2D (transverse spatial) + 1D (longitudinal momentum) coordinate space images from exclusive scattering

Transverse Momentum Distributions (TMDs)

Generalized Parton Distributions (GPDs)

3-D Imaging of Quarks and Gluons

$W(x, b_T, k_T)$

Momentum space

$\int d^2 b_T$

$\int d^2 k_T$

Coordinate space

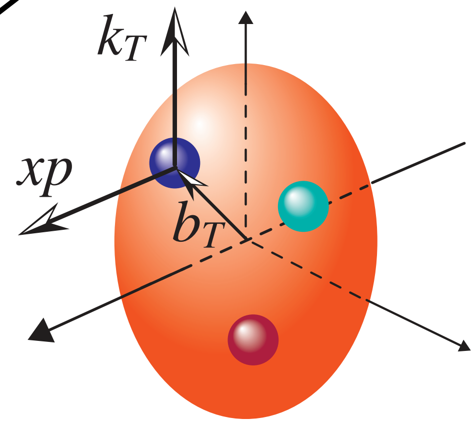

Quarks

$f(x, k_T)$

$f(x, b_T)$

Gluons

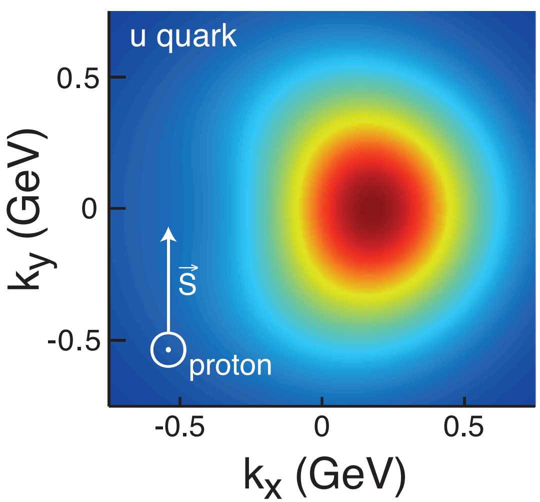

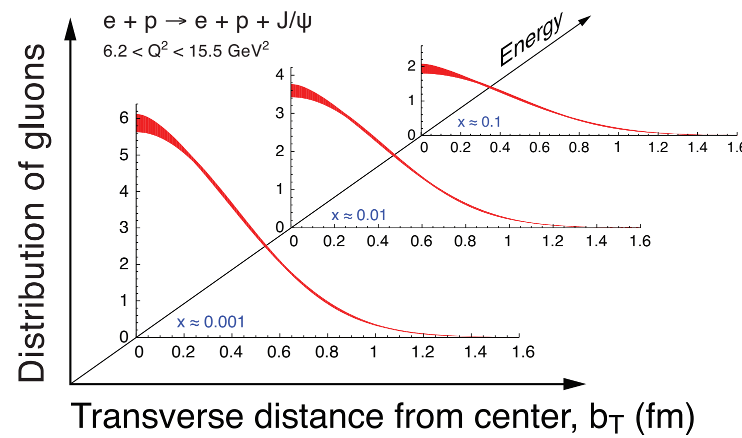

Spin-dependent 2D (transverse spatial) + 1D (longitudinal momentum) coordinate space images from exclusive scattering

Transverse Momentum Distributions (TMDs)

Generalized Parton Distributions (GPDs)

3-D Imaging of Quarks and Gluons

$W(x,b_T,k_T)$

Momentum space

$\int d^2b_T$

$\int d^2k_T$

Coordinate space

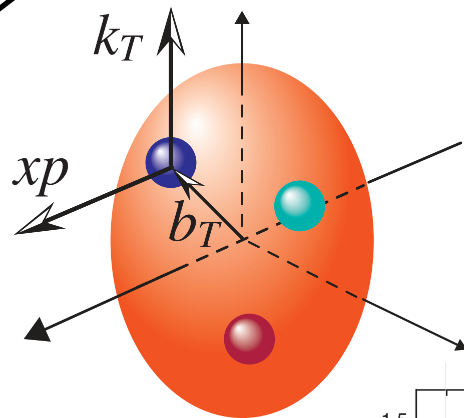

Quarks

$f(x,k_T)$

$f(x,b_T)$

Gluons

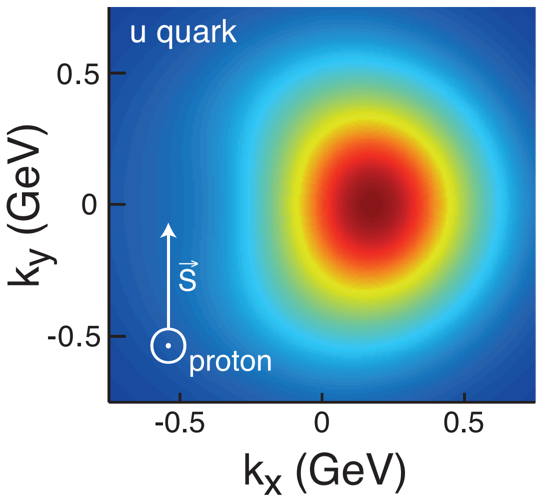

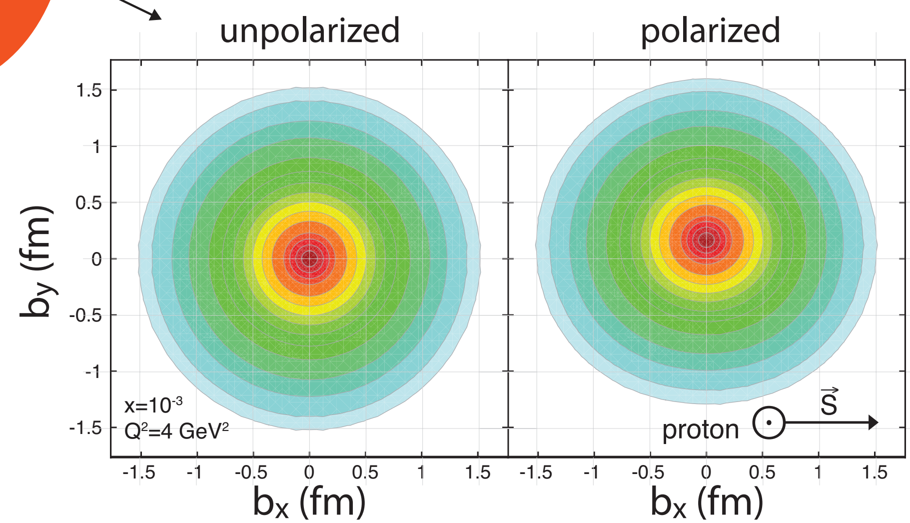

Transverse Momentum Distributions (TMDs)

Generalized Parton Distributions (GPDs)

3-D Imaging of Quarks and Gluons

$W(x, b_T, k_T)$

Momentum space

$\int d^2 b_T$

$\int d^2 k_T$

Coordinate space

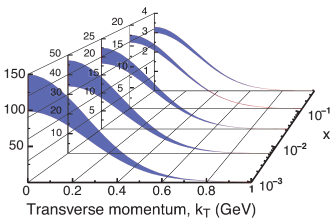

$f(x, k_T)$

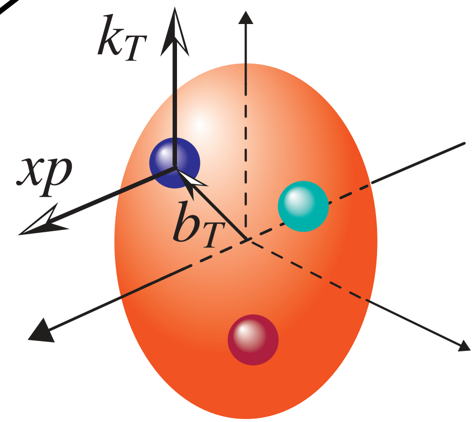

$f(x, b_T)$

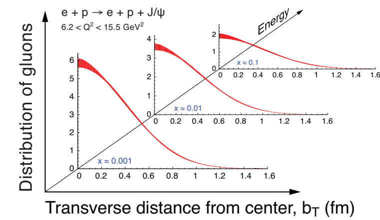

$\int d^2 k_T$

$\int d^2 b_T$

$f(x)$

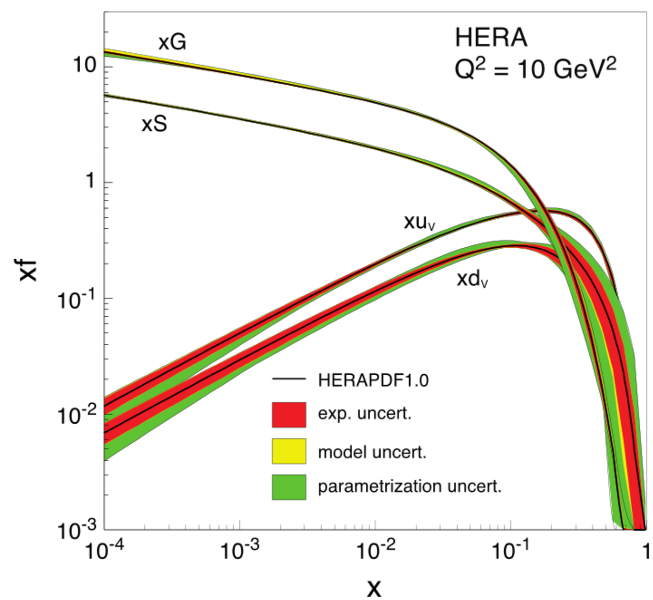

3-D Imaging of Quarks and Gluons

Imaging is **big** part of EIC program:

- luminosity and energy hungry
- multi-year program
- GPD: measured via DVCS and diffractive vector meson production
- TMD: semi-inclusive DIS
- For more details: see lectures by Alexei Prokudin and Anselm Vossen (Hadron Structure)

Diffractive Virtual Compton Scattering (DVCS)

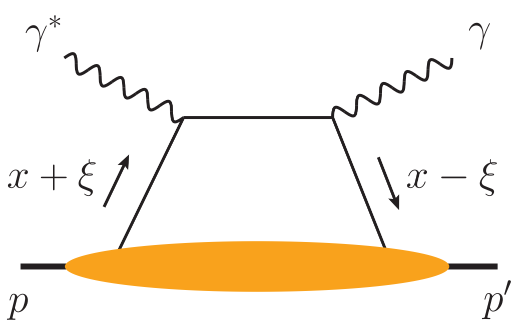

Diffractive Exclusive Vector Meson Production

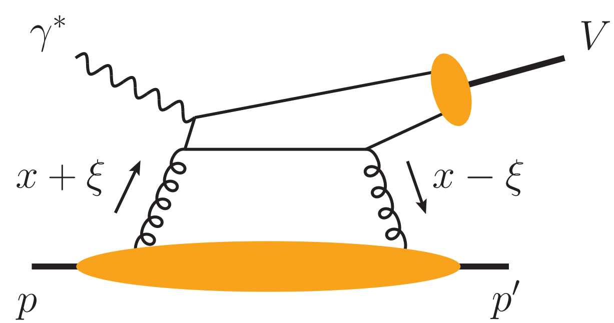

8.3. Structure Functions and Nuclear PDFs in eA Collisions

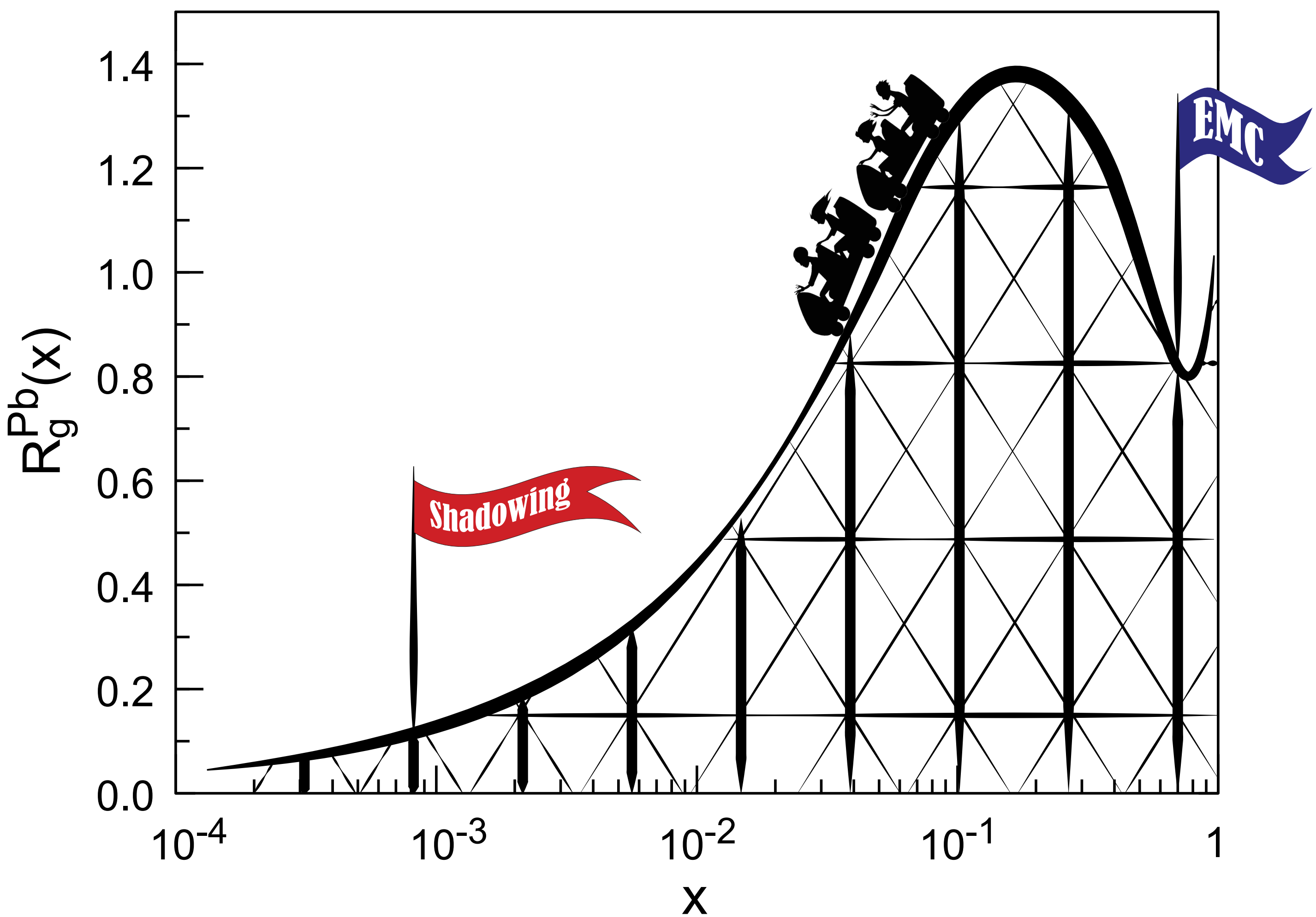

Nuclear PDFs (nPDFs)

Goal: Describe initial state of nuclei

For nuclei typically formulated as ration of structure fct A/p

$$R^A_{i=g,u,d,\dots}(x,Q^2) = \frac{f_i^A(x,Q^2)}{f_i^p(x,Q^2)}$$

3 distinguished regions:
- shadowing
- anti-shadowing
- EMC effect region

none is understood

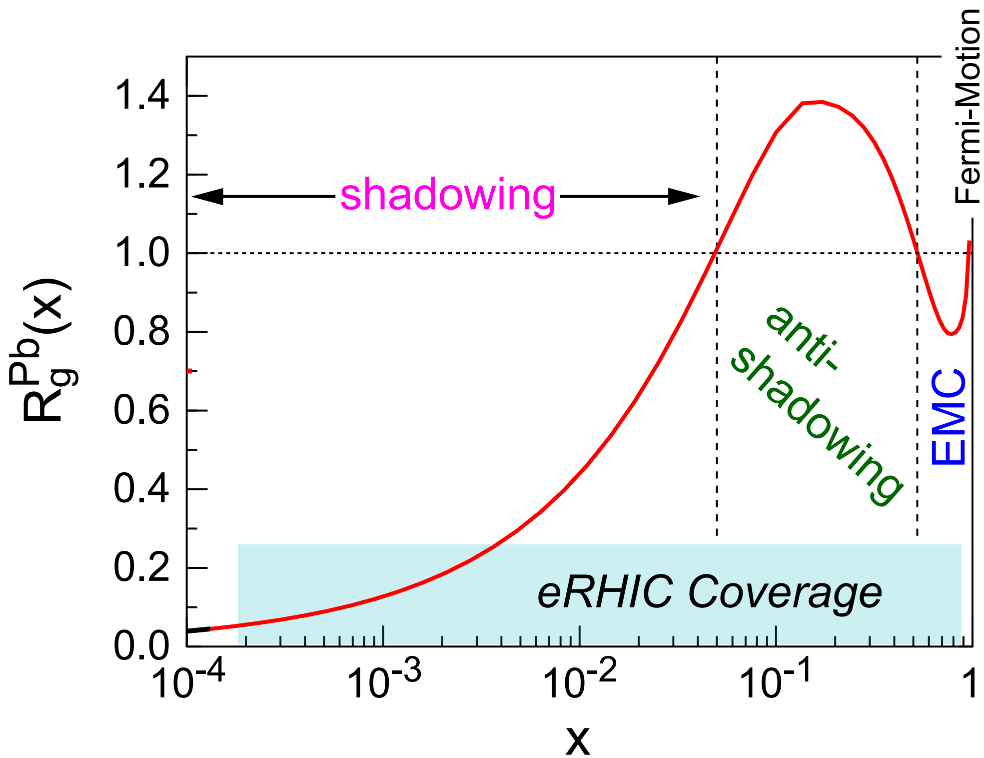

nPDFs are of interest in their own right but are also important for other fields (Heavy-Ions, Cosmic Rays etc)

Nuclear PDFs

nPDFs less well known due to lack of data

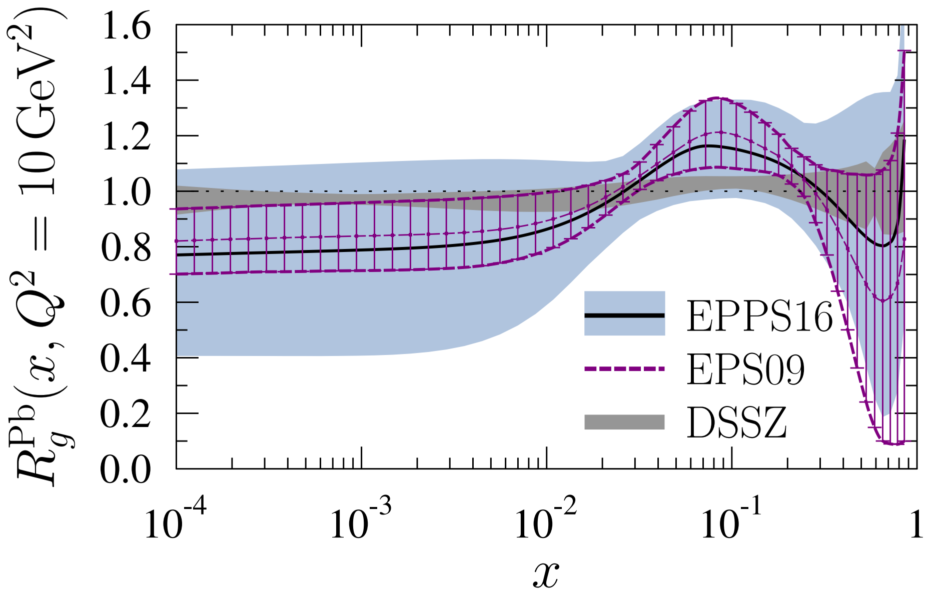

nPDF fits typically performed on reduced cross-section

$$\sigma_{\text{red}}(x, Q^2) = F_2(x, Q^2) - \left(\frac{y^2}{1+(1-y)^2}\right) F_L(x, Q^2)$$

Theory/models have to be able to describe the structure functions and their evolution

- DGLAP:
  - predicts Q^2 but not A and x dependence
- Saturation models (JIMWLK):
  - predict A and x dependence but not Q^2
- Need: large Q^2 lever-arm for fixed *x*, A-scan

e+A: Aim at extending our knowledge on structure functions into the realm where gluon saturation (higher twist) effects emerge
$\Rightarrow$ different evolution (JIMWLK)

EIC: Structure Functions in eA

EIC pseudo-data

- F_L, F_2, σ_{red}, F_2^{cc} values from EPPS16
- Errors (sys and stat.) from simulations for $\int L dt = 10\ fb^{-1}/A$

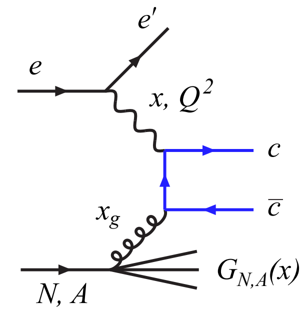

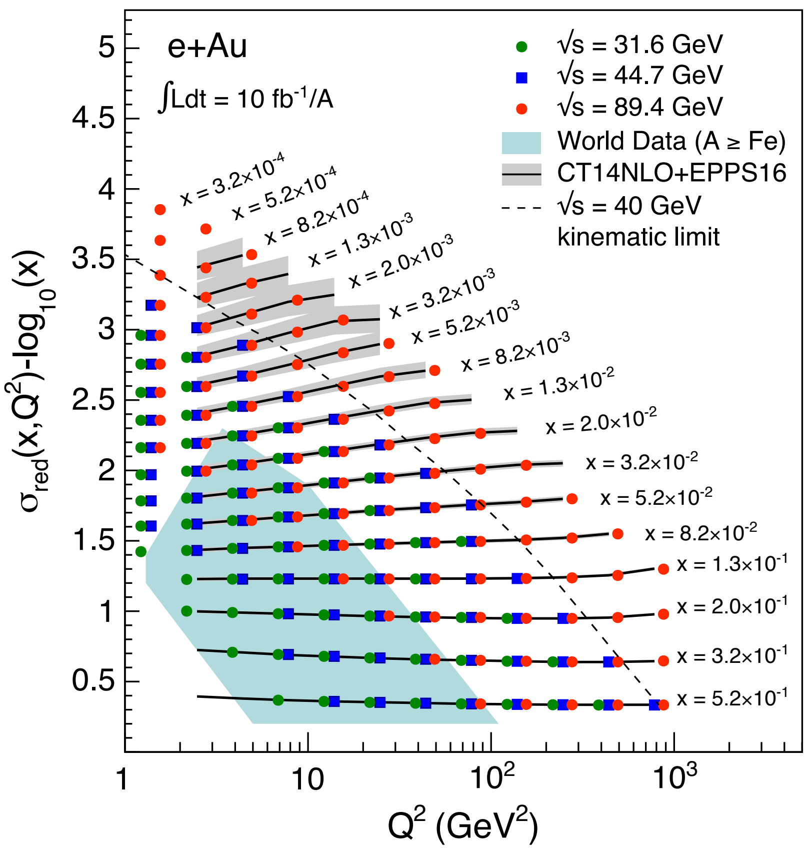

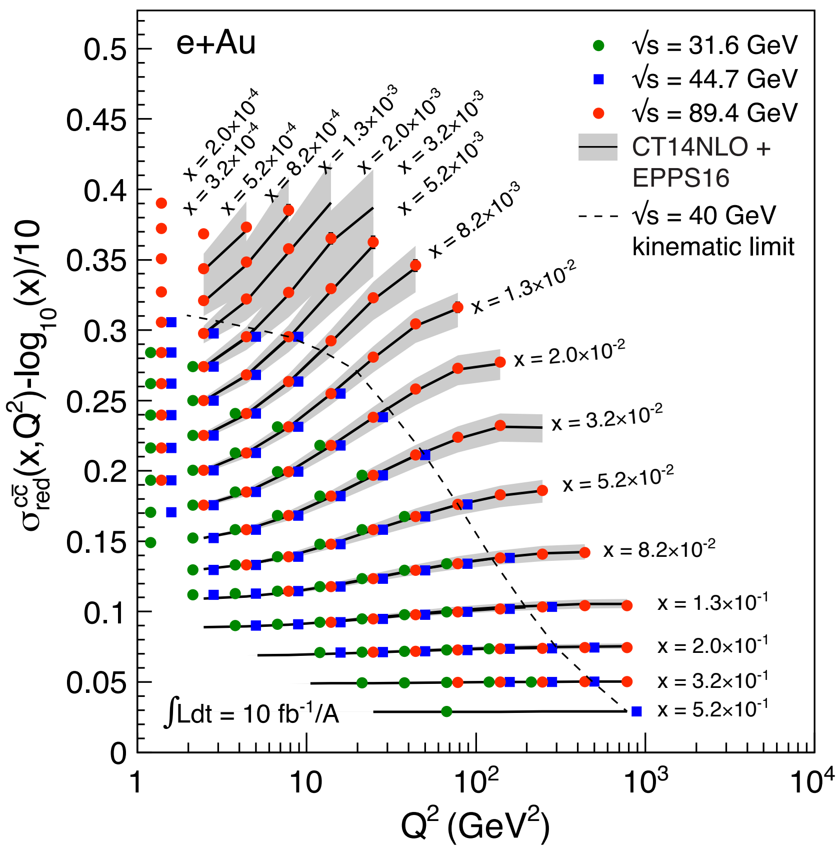

arXiv:1708.01527, 1708.05654

EIC: F_L Structure Function

- F_L probes glue more directly
- F_L is small and requires running at different √s and thus has larger systemic uncertainties than F_2

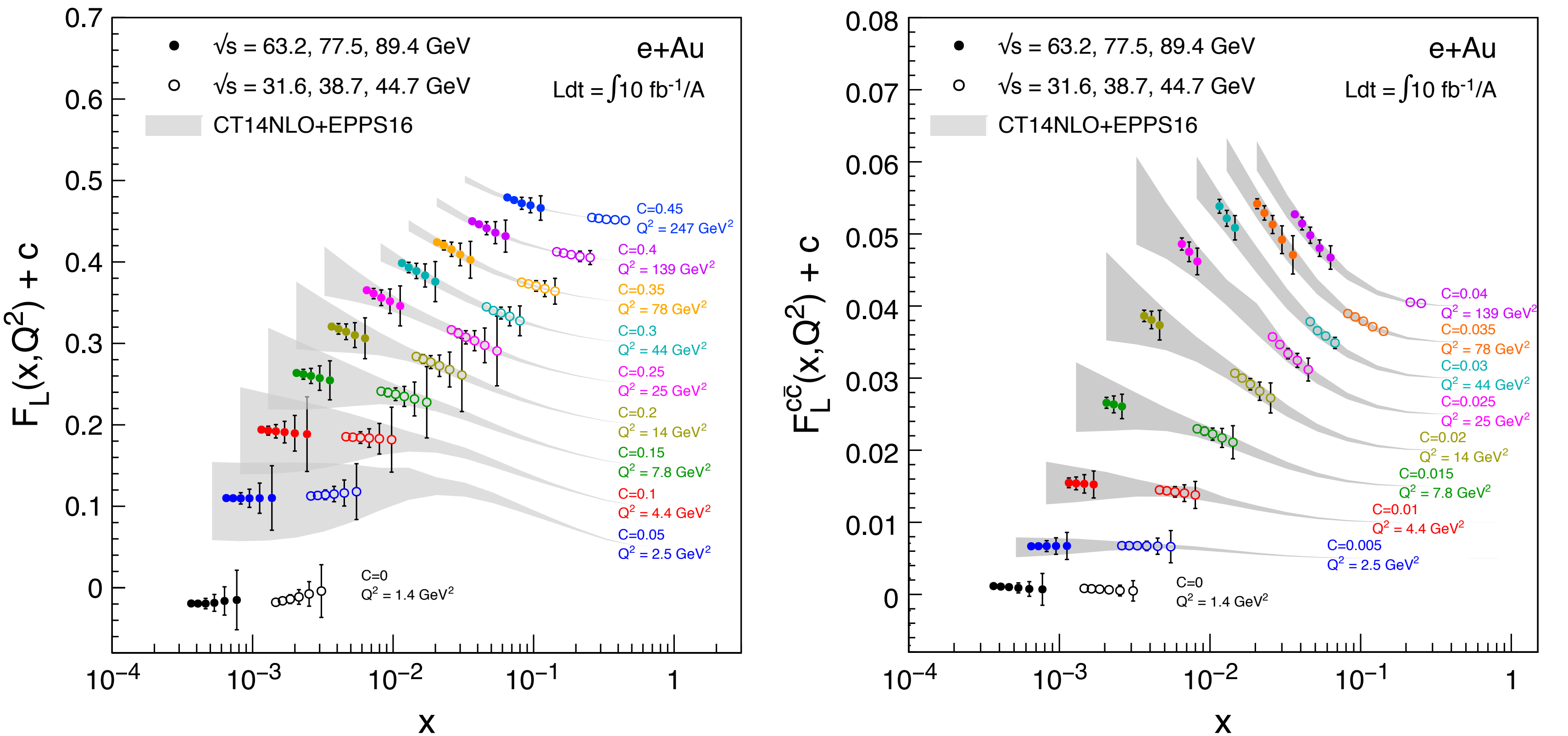

- Dramatic improvements with EIC at highest energy

EIC's Impact on nPDFs (R_{glue})

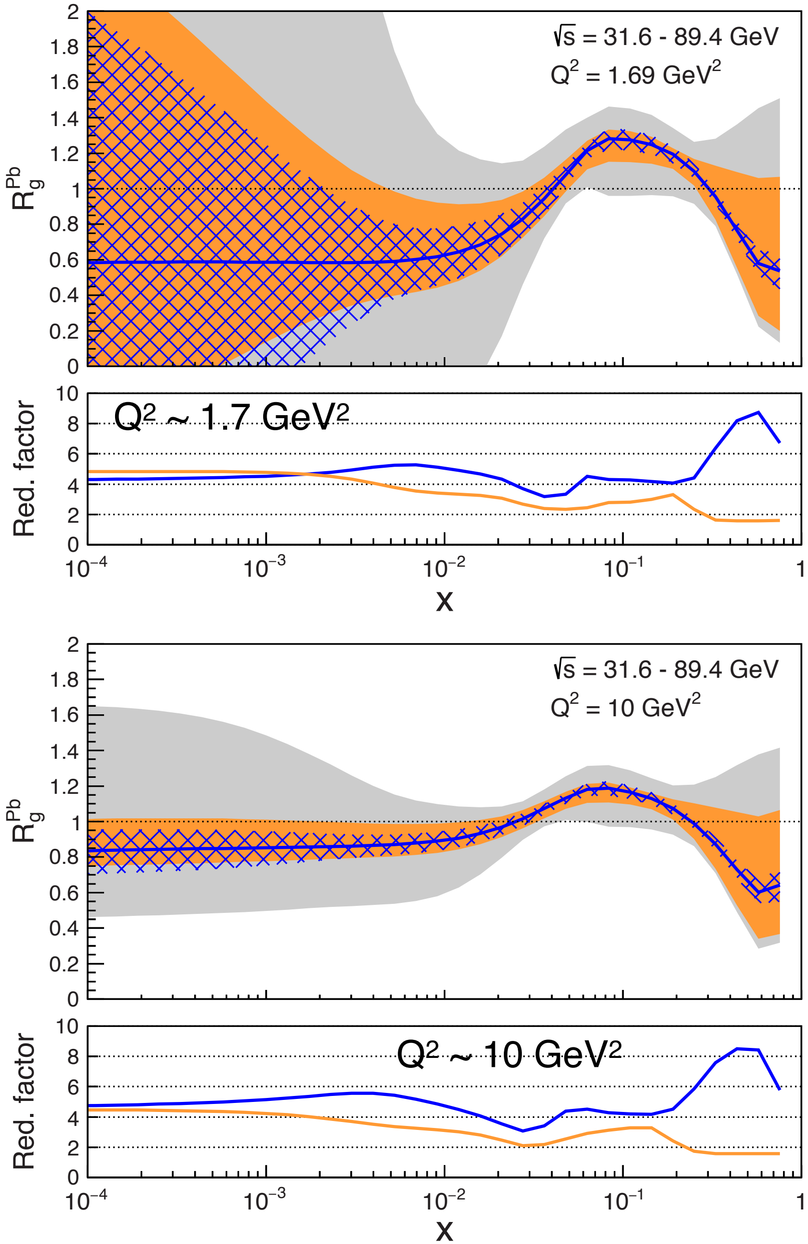

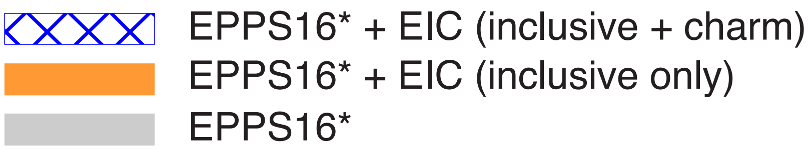

- Improves uncertainties substantially out to 10^{-4}
- Shrinks uncertainty band by factors 4-8
- Charm: no additional constraint at low-x but dramatic impact at large-x

arXiv:1708.01527

8.4 Dihadron Correlations

Dihadron Correlations

Dihadron correlation as a probe to saturation.

Saturation models predict suppression of away-side peak

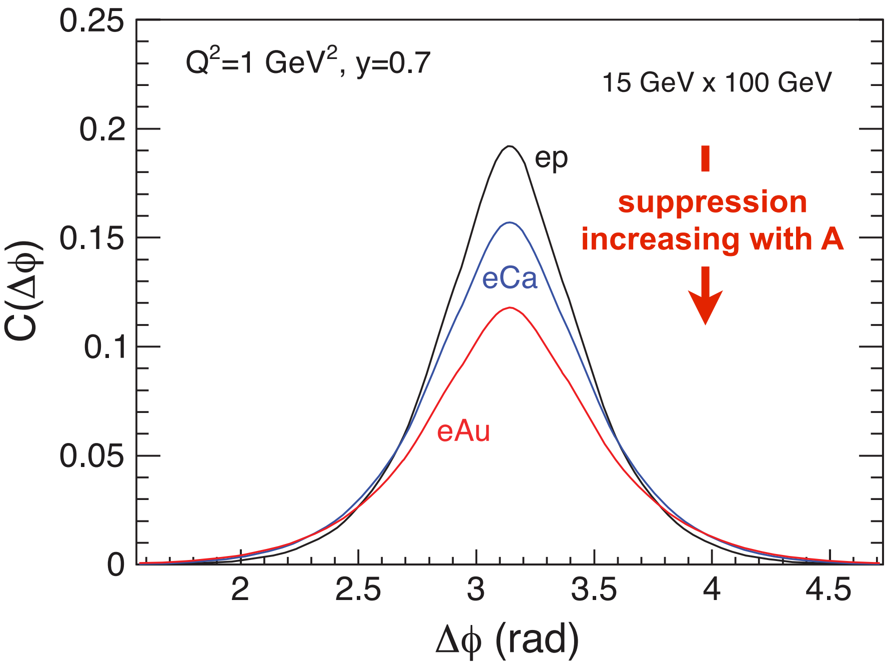

Experimental Simple Measurement

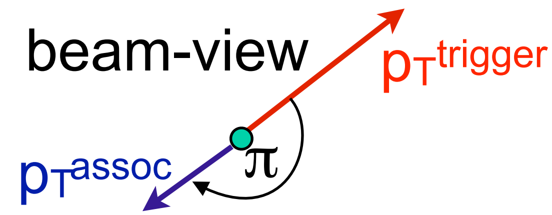

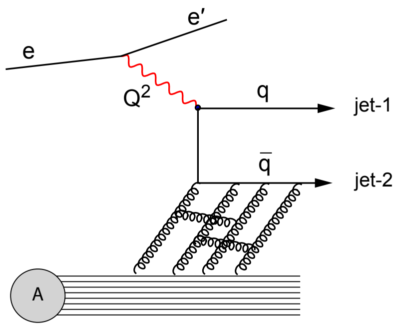

Interpretation: decorrelation due to interaction with low-x gluonic matter

- Predicted [C. Marquet, 09] as important hint of saturation
- Robust calculations available (Albacete, Dominguez, Lappi, Marquet, Stasto, Xiao) including Sudakov resummation in dijet processes

Dihadron Correlations

Dihadron correlation as a probe to saturation.

Saturation models predict suppression of away-side peak

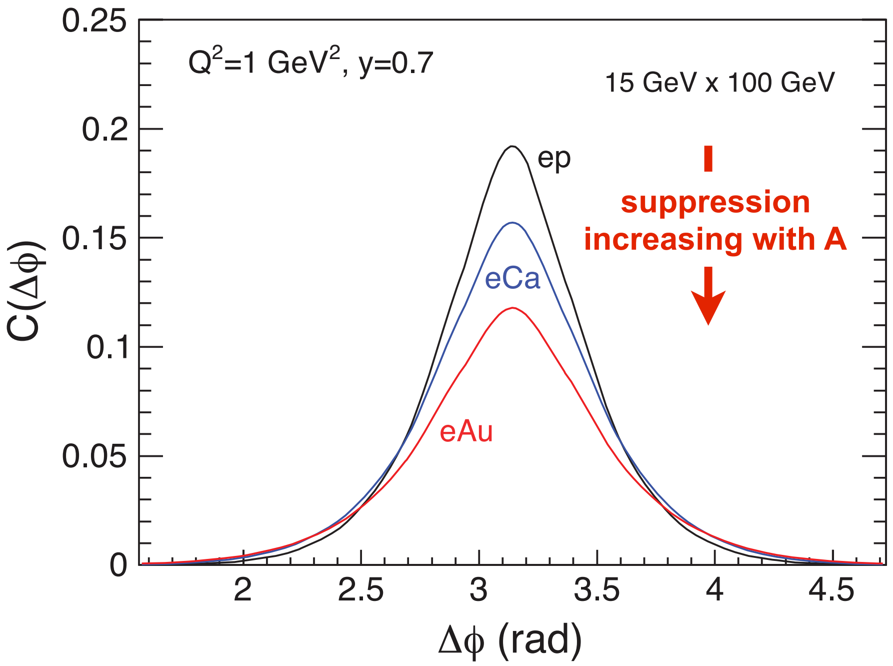

Experimental Simple Measurement

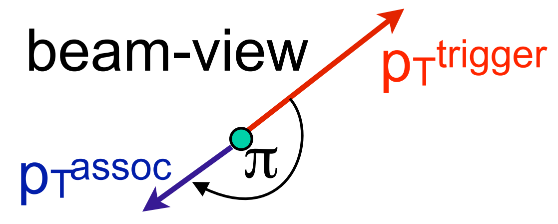

Interpretation:
decorrelation due to interaction with low-x gluonic matter

- Predicted [C. Marquet, 09] as important hint of saturation
- Robust calculations available (Albacete, Dominguez, Lappi, Marquet, Stasto, Xiao) including Sudakov resummation in dijet processes

Reminder: Dihadrons at RHIC

p/d+Au at forward rapidities

- Tantalizing hint for initial state suppression as predicted by CGC

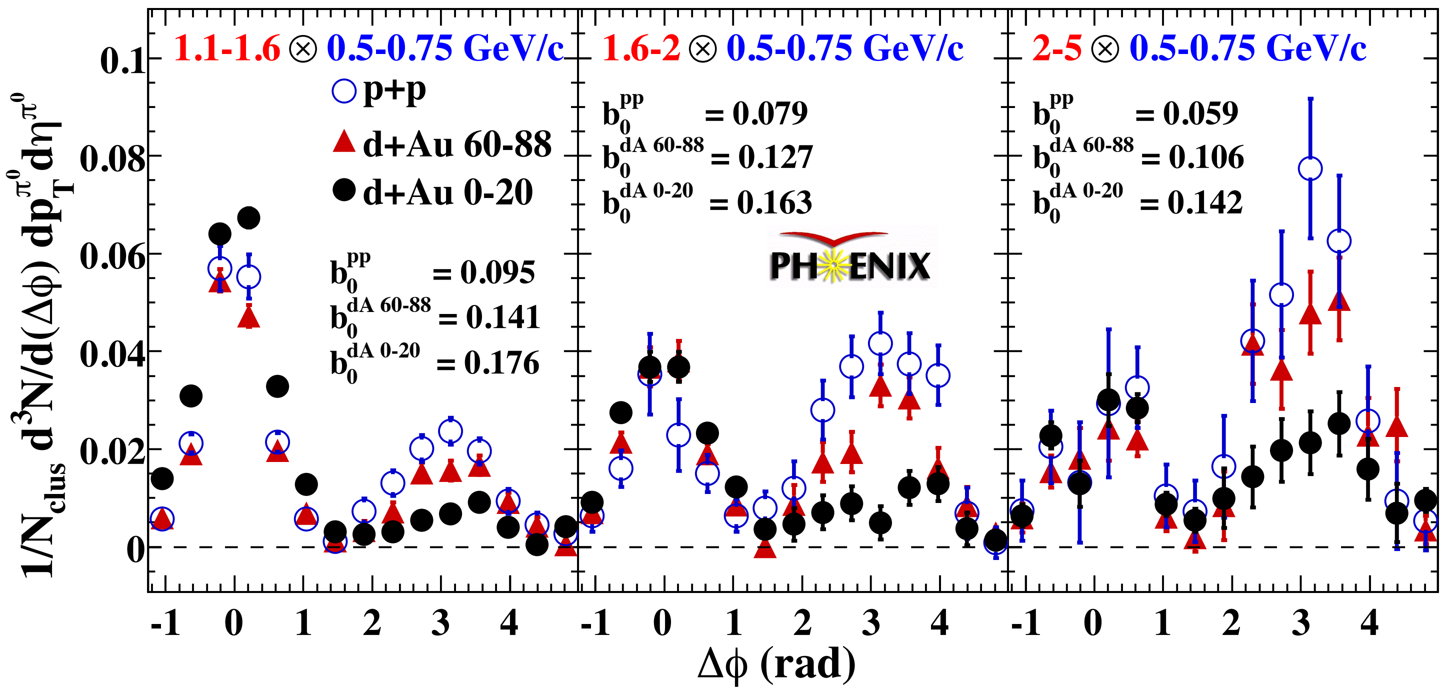

Reminder: Dihadrons at RHIC

p/d+Au at forward rapidities

- Tantalizing hint for initial state suppression as predicted by CGC

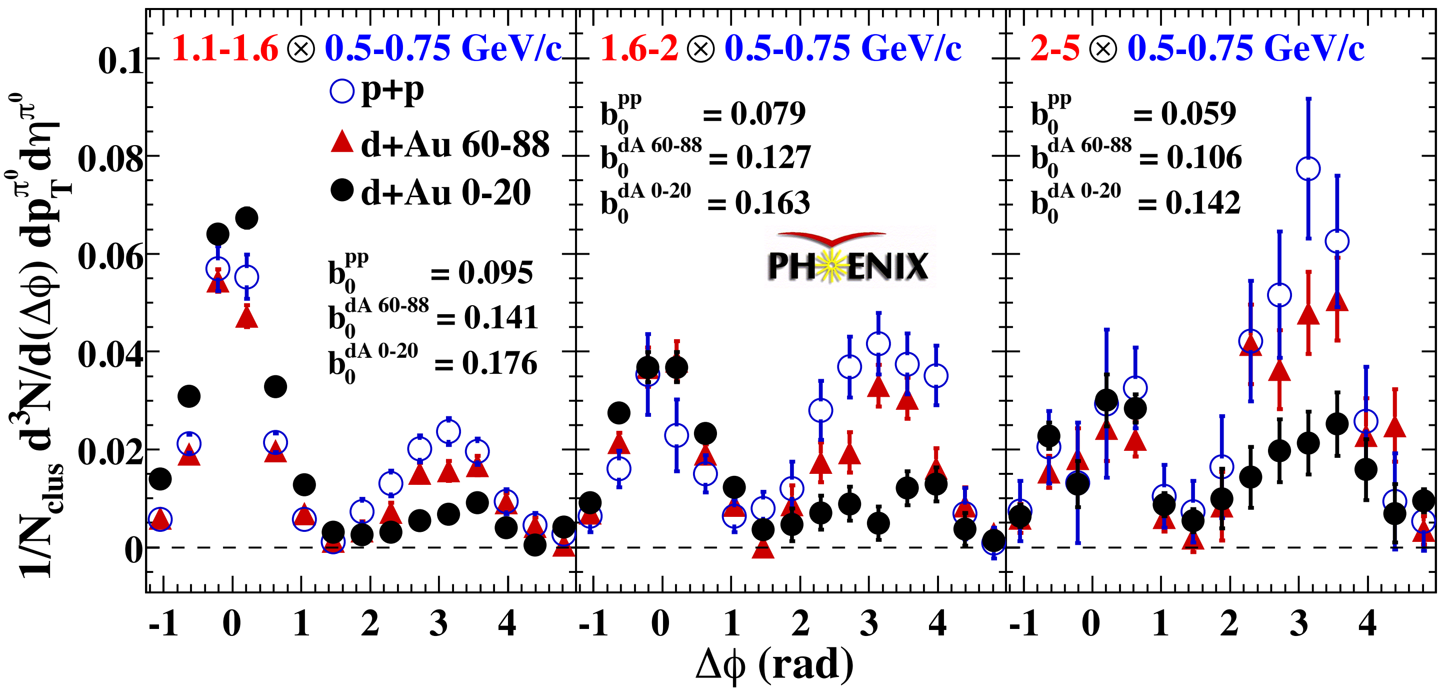

- Cannot assure that effect is initial state in p/d+A
- Large background, no access to process kinematics (x_g)

⇒ e+A

EIC Simulation Results: Dihadrons

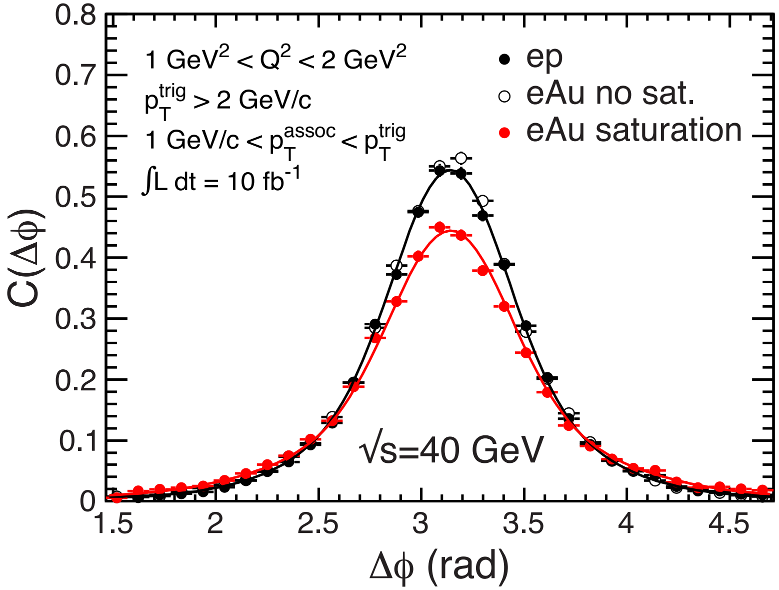

EIC Simulation Results: Dihadrons

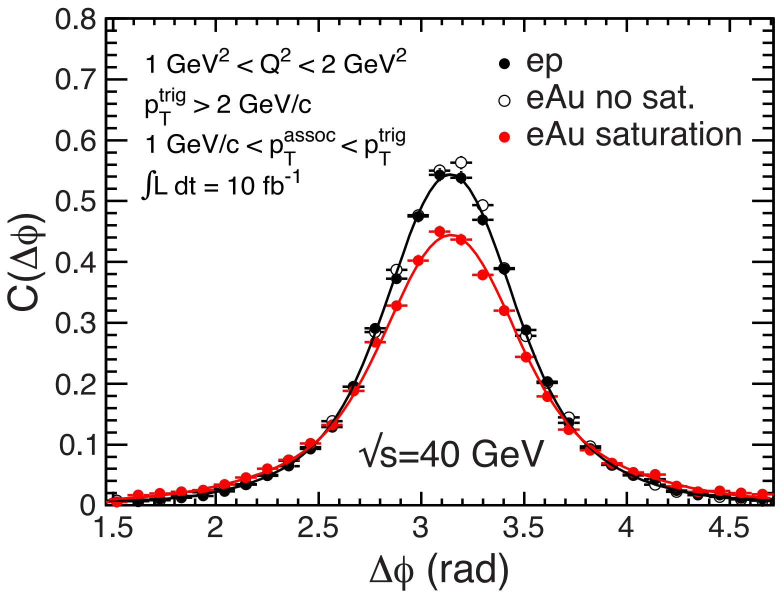

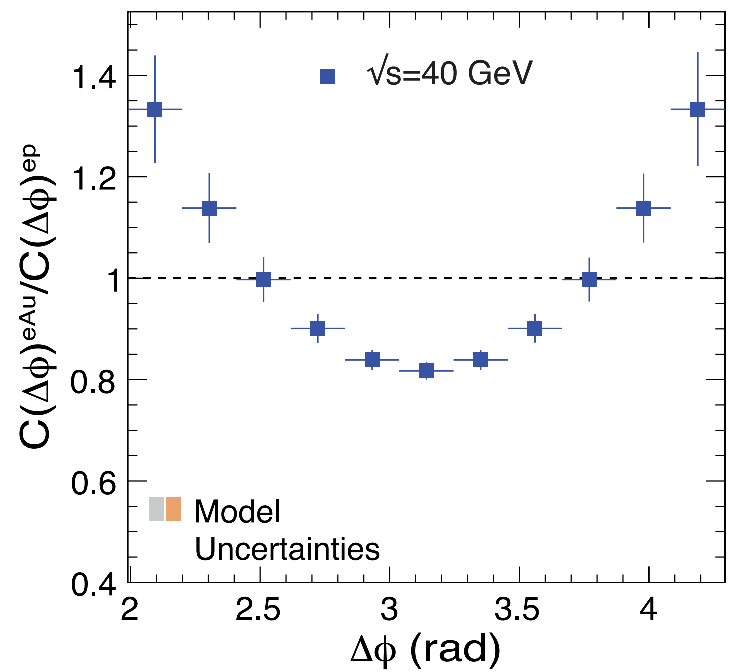

Zheng et al., PRD89 (2014) 074037; BNL-114111-2017, arXiv:1708.01527

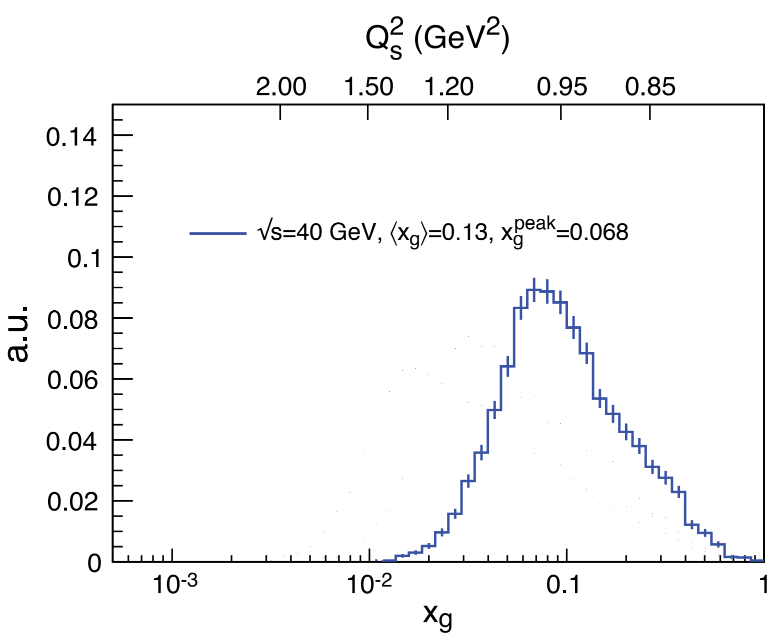

EIC Simulation Results: Dihadrons

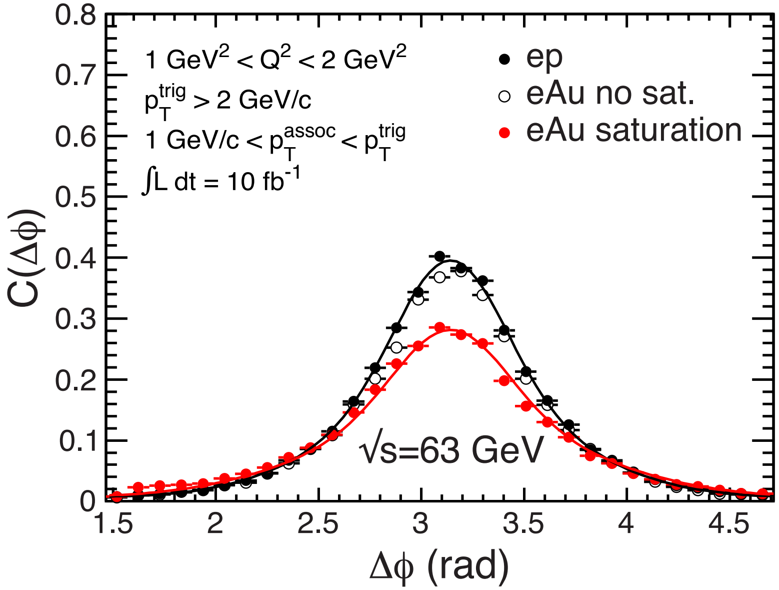

Ratio

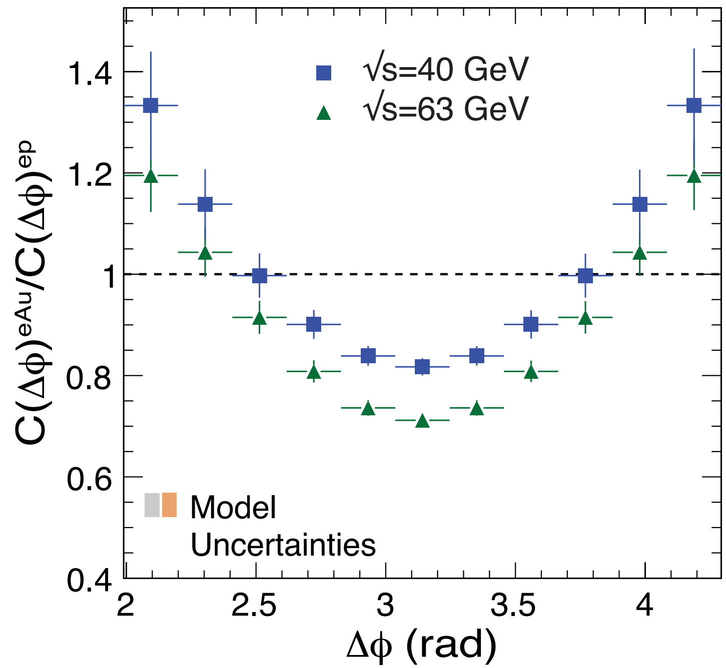

Zheng et al., PRD89 (2014) 074037; BNL-114111-2017, arXiv:1708.01527

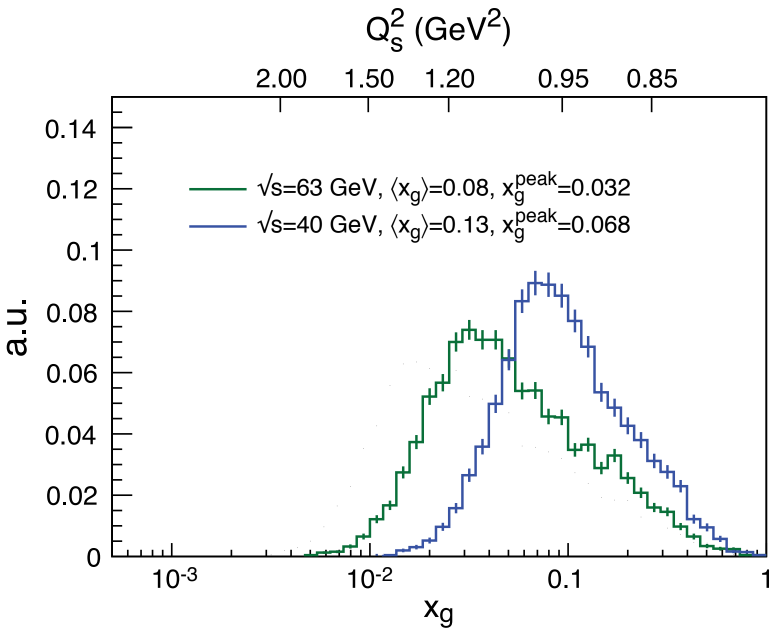

EIC Simulation Results: Dihadrons

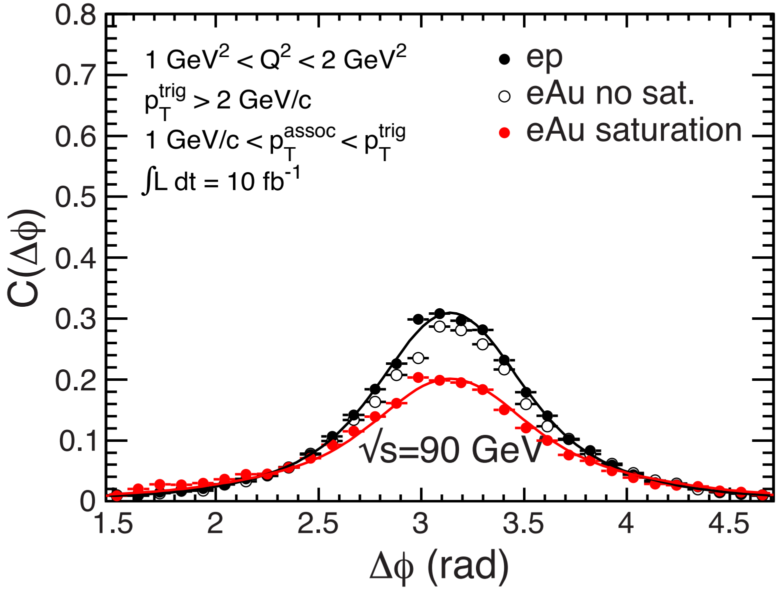

Ratio

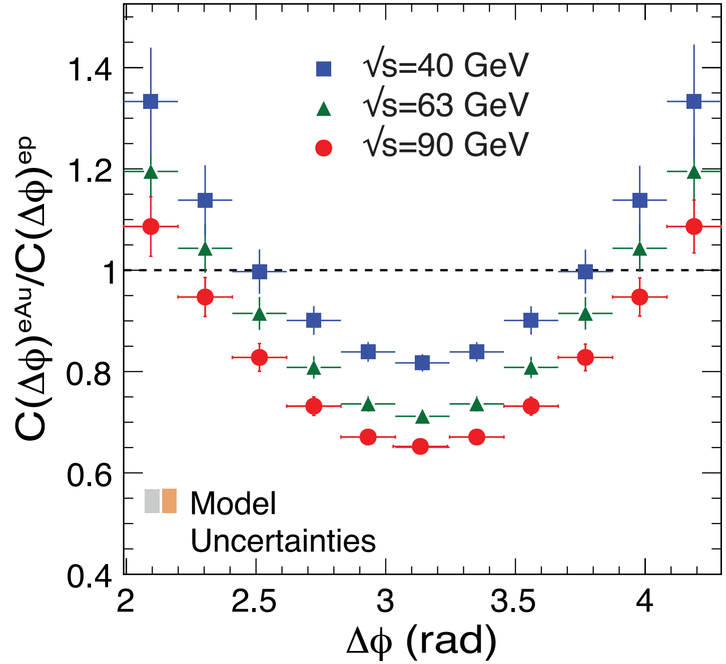

Zheng et al., PRD89 (2014) 074037;
BNL-114111-2017, arXiv:1708.01527

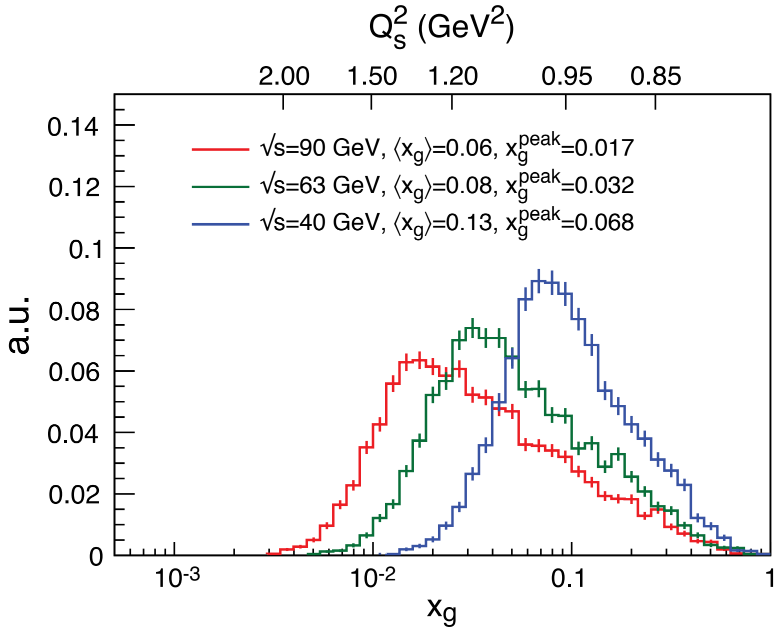

- Clear saturation signature
  - Allows us to extract the spatial multi-gluon correlations
- Similar Dijet Correlations
  - Unique measurement of WW Gluon Distributions (nTMDs)

8.5 Diffractive Physics in eA

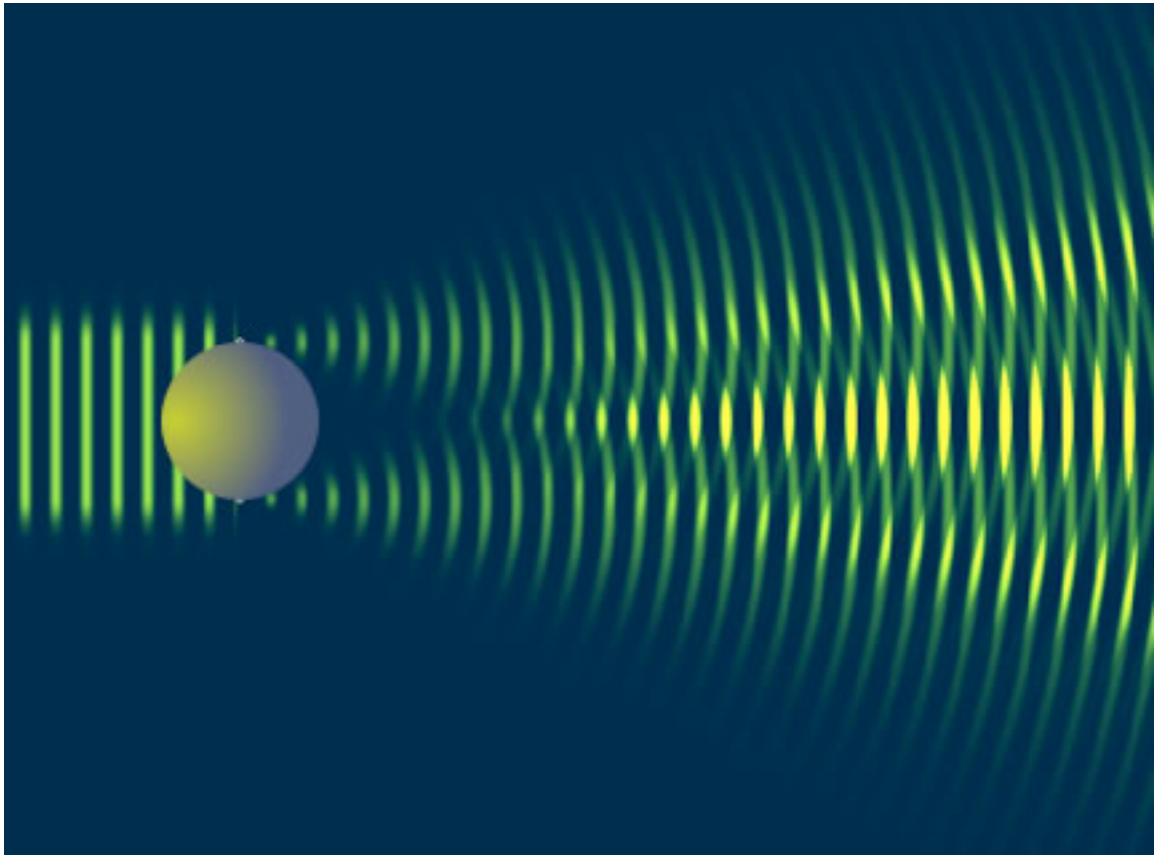

Hard Diffraction: What is It?

A DIS event (theoretical view)

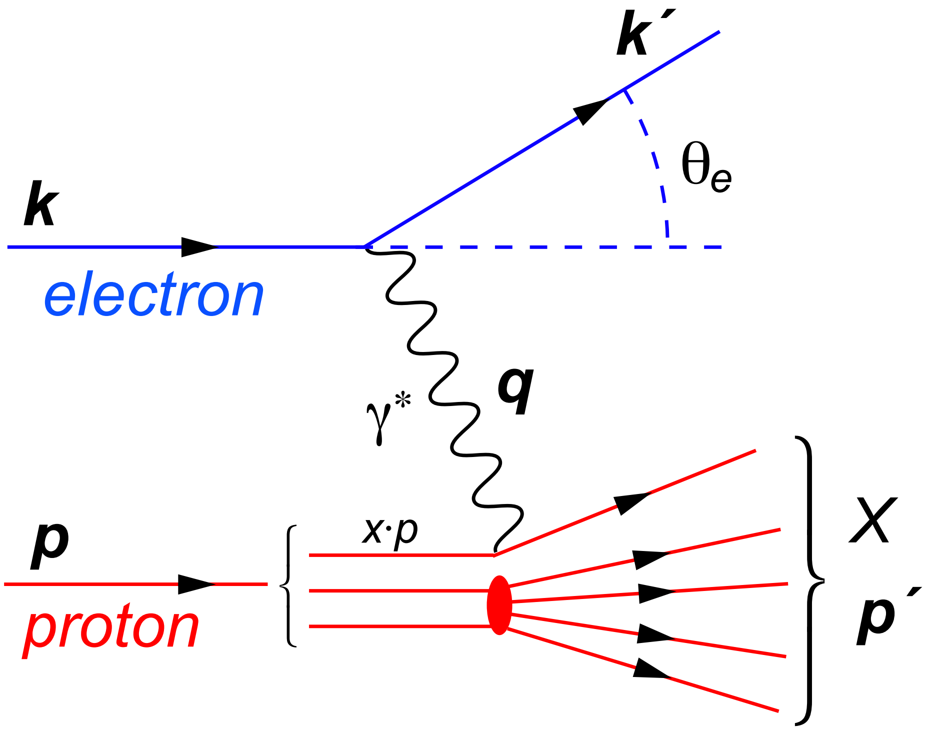

Hard Diffraction: What is It?

A DIS event (experimental view)

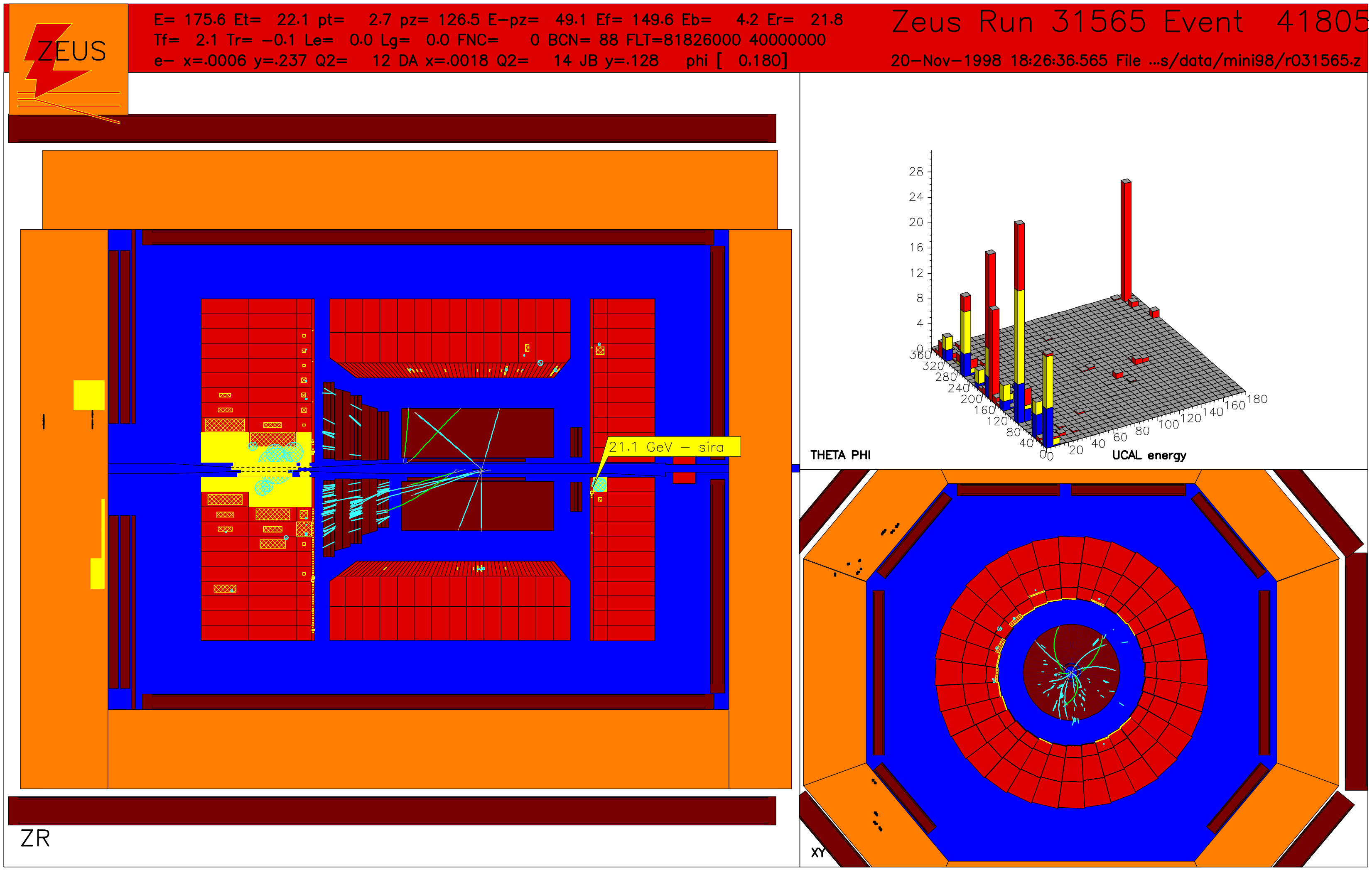

Hard Diffraction: What is It?

A DIS event (experimental view)

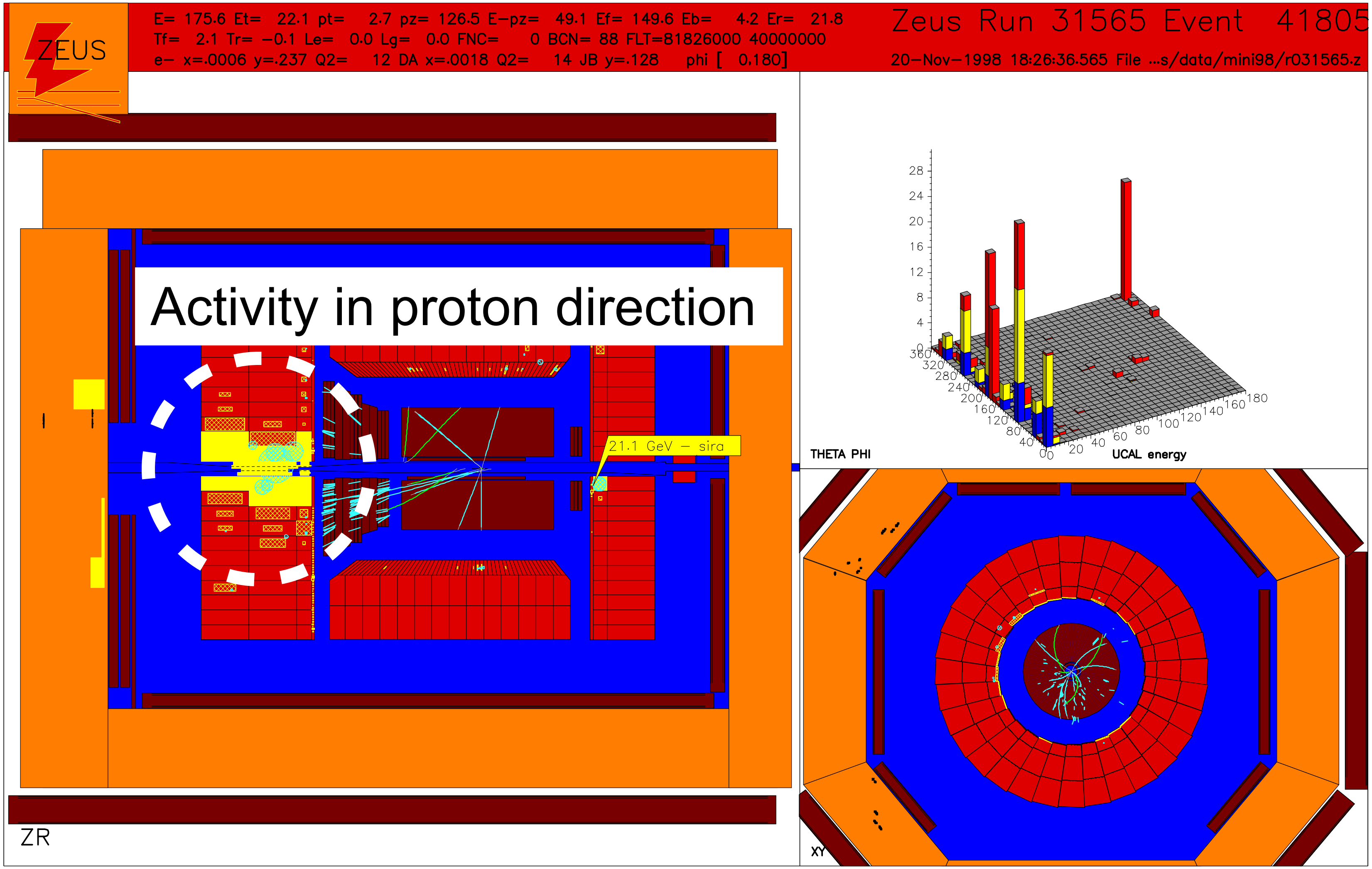

Hard Diffraction: What is It?

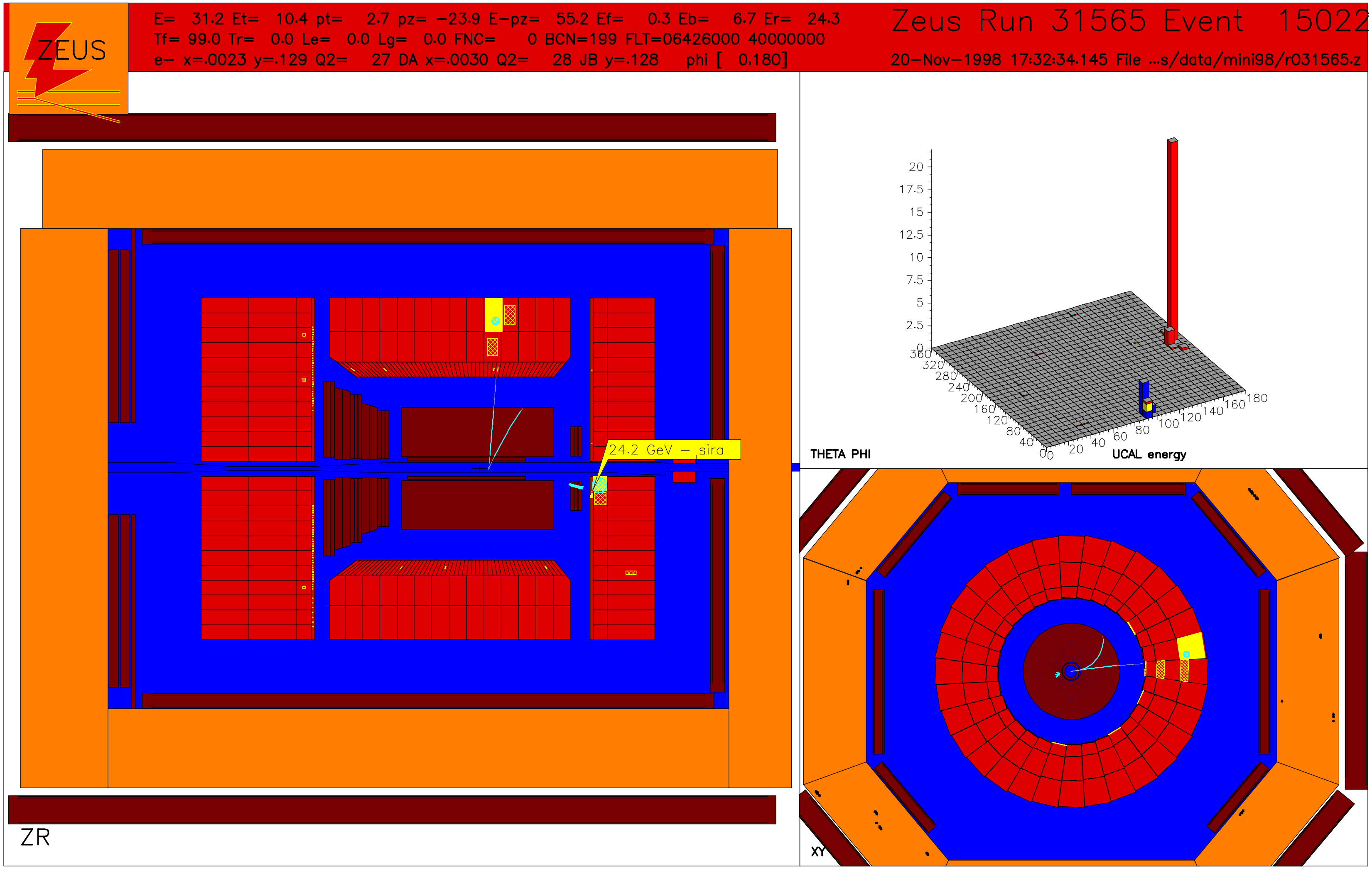

Hard Diffraction: What is It?

A diffractive event (experimental view)

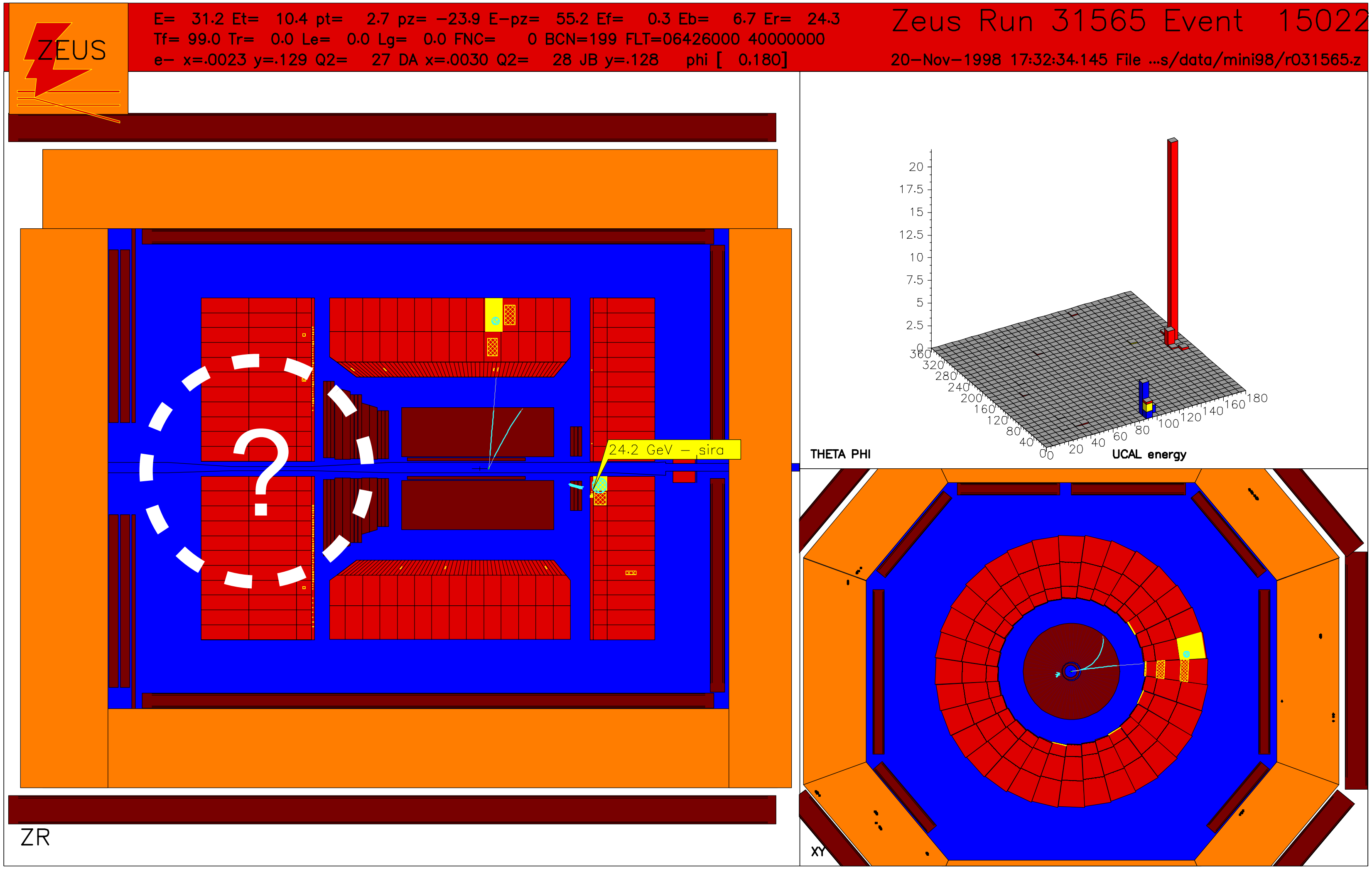

Hard Diffraction: What is It?

A diffractive event (theoretical view)

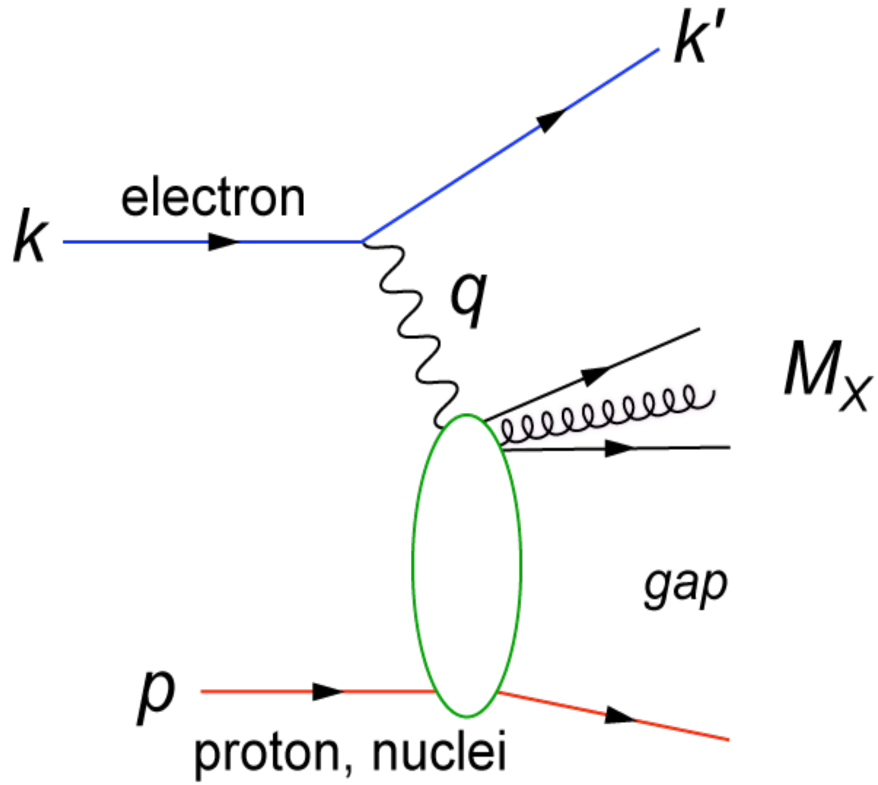

- HERA: large fraction of diffractive events (15% of total DIS rate)

Diffraction for the 21st Century

Diffractive physics will be a major component of the e+A program at an EIC

HERA: $\sigma_{diff}/\sigma_{tot} \sim 14\%$

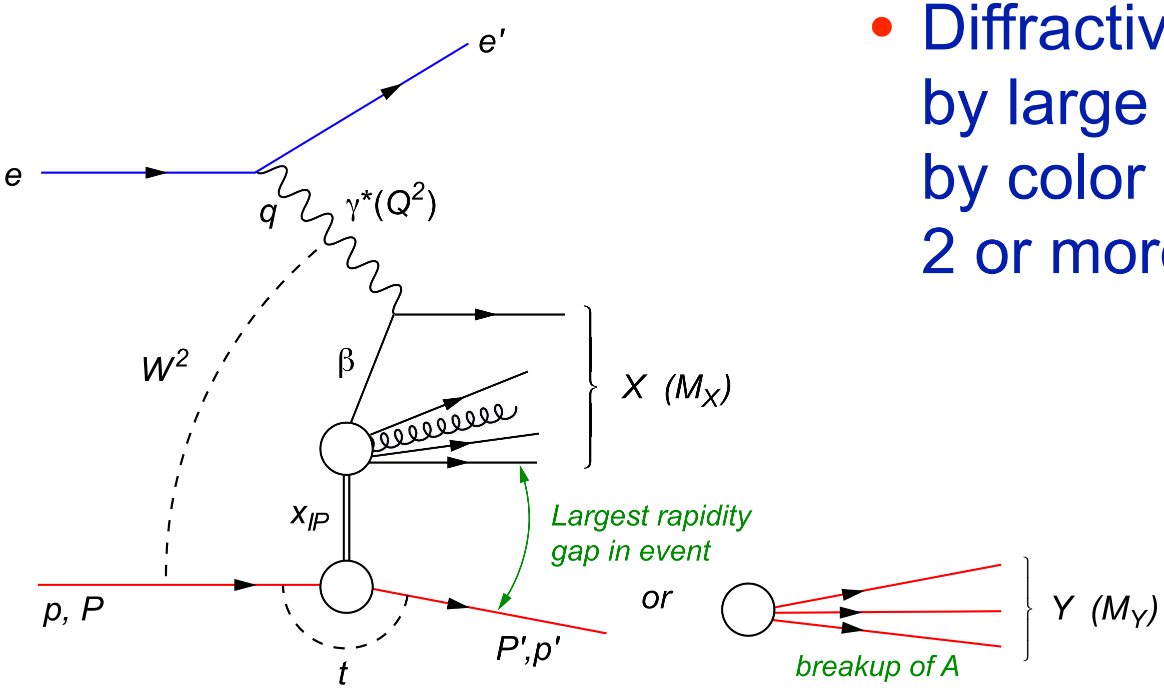

- Diffractive event characterized by large rapidity gap mediated by color neutral exchange (e.g. 2 or more gluons) aka Pomeron

coherent
p/A stays intact

incoherent
p/A breaks up

t: momentum transfer squared $(\mathbf{p}-\mathbf{p'})^2$

M_X: mass of diffractive final-state

Why Is Diffraction So Important?

Recall: diffractive pattern in optics

Position of minima θ_i related to size R of screen

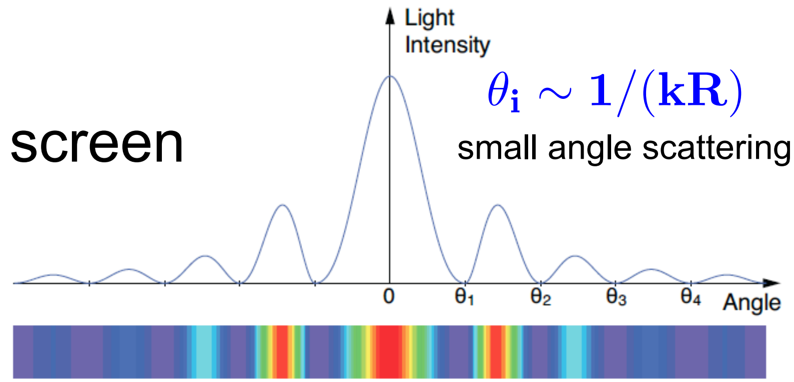

Similarly: in coherent (elastic) scattering dσ/dt resembles diffractive pattern where $|t| \approx k^2\theta^2$

Crucial differences:

- target not always "black disc"
  - sensitivity to "size" of probe / onset of black disc limit
- incoherent (inelastic) contribution

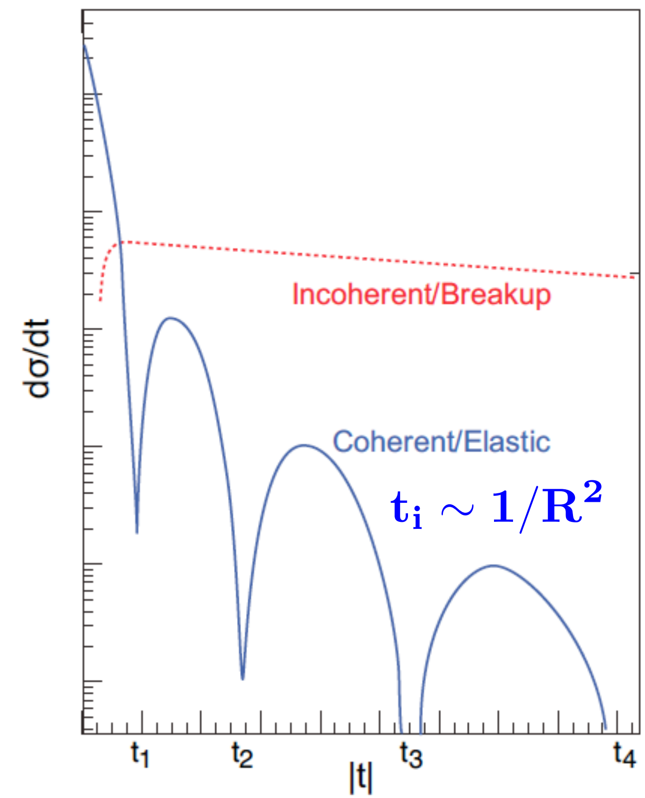

High Sensitivity to g(x,Q^2)

Diffraction is most precise probe of non-linear dynamics in QCD

Example: Exclusive diffractive production of a vector meson

$$\gamma^* p \rightarrow V p'$$
$$\gamma^* A \rightarrow V A'$$

$$\mathbf{d\sigma \sim [g(x)]^2}$$

Dipole Model

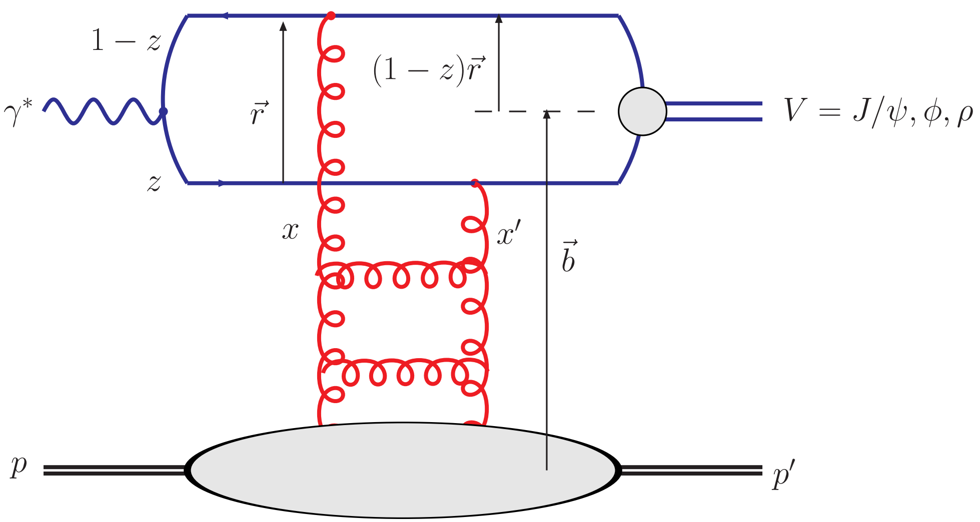

- High sensitivity to gluon density: $\sigma \sim [g(x,Q^2)]^2$ due to color-neutral exchange

Exclusive Diffractive Vector Meson

- *t* can be measured in e+p with a forward spectrometer measuring the scattered p
- in e+A this is not possible. A' stays in the beam pipe.
- Only process where this is possible is VM production.

$$t = (\boldsymbol{p}_A - \boldsymbol{p}_{A'})^2 = (\boldsymbol{p}_{\mathrm{VM}} + \boldsymbol{p}_{e'} - \boldsymbol{p}_e)^2$$

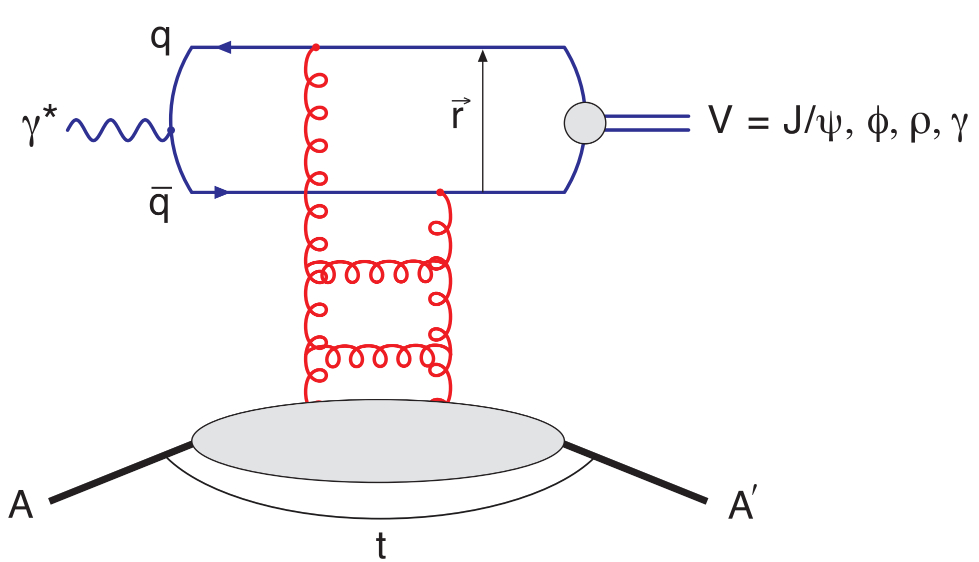

Sartre 1: Diffractive Vector Meson Production

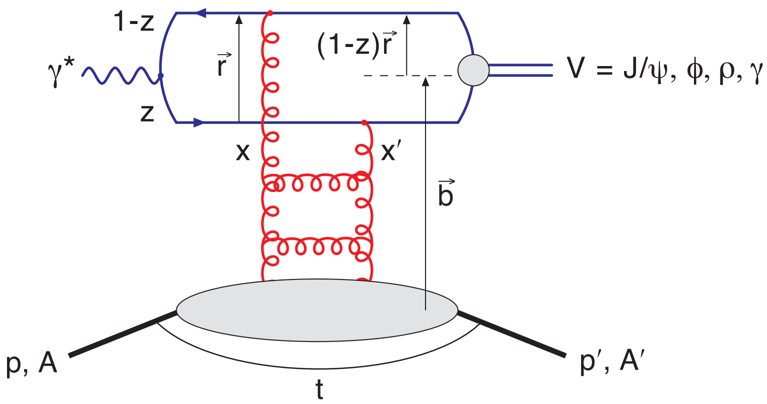

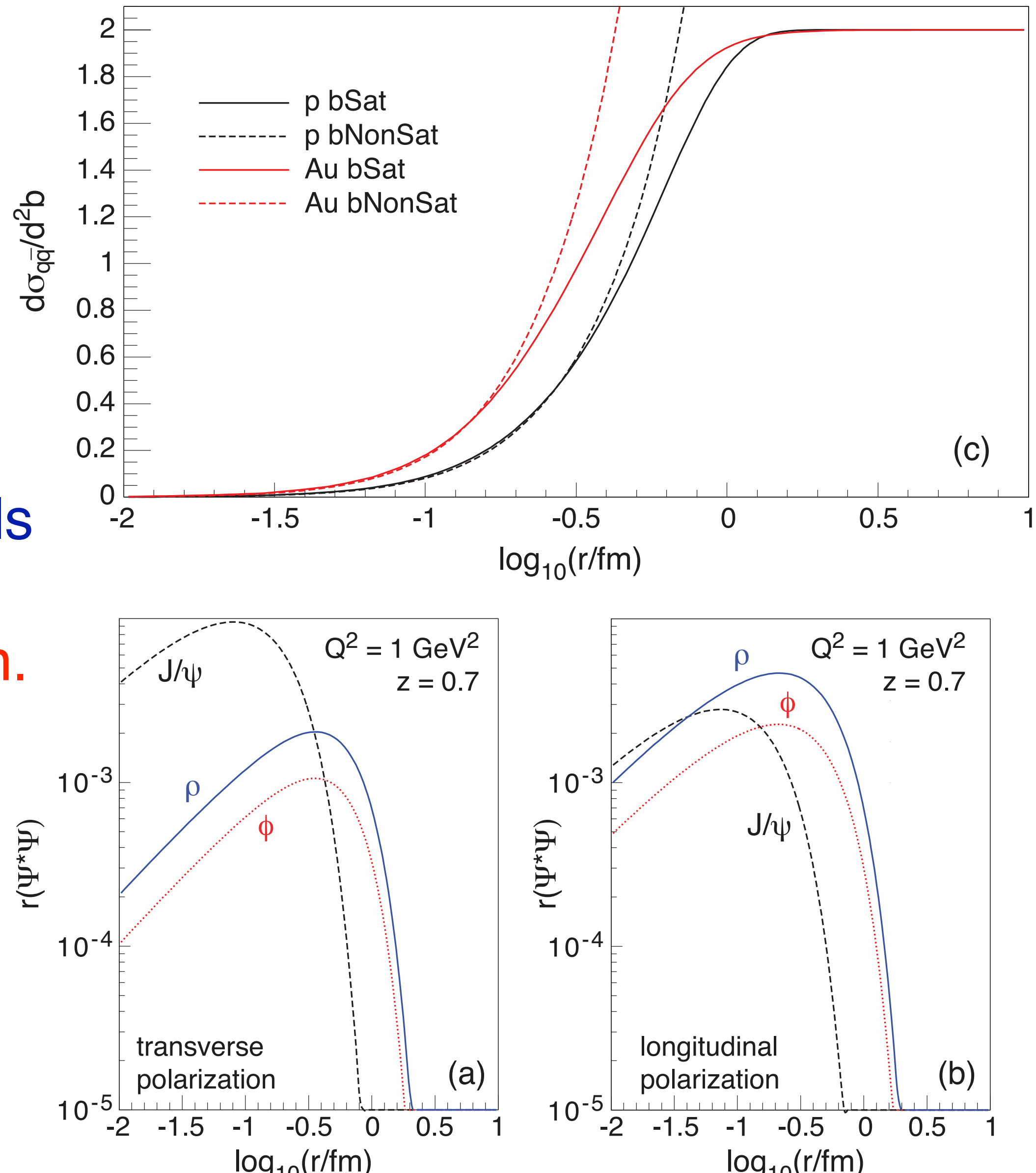

Wave overlap function $\Psi^*\Psi$ falls steeply for large dipole radii

- J/ψ not sensitive to saturation.
- Need to look at ϕ, or ρ that "see" more of the dipole amplitude

$$\mathcal{A}_{T,L}^{\gamma^* p\rightarrow Vp}(x,Q,\Delta) = i\int \mathrm{d}r \int \frac{\mathrm{d}z}{4\pi}\int \mathrm{d}^2\mathbf{b}(\Psi_V^*\Psi)(r,z)$$
$$\times 2\pi r J_0([1-z]r\Delta)e^{-i\mathbf{b}\cdot\Delta}\frac{\mathrm{d}\sigma_{q\bar{q}}^{(p)}}{\mathrm{d}^2\mathbf{b}}(x,r,\mathbf{b})$$

Sartre 1: Diffractive Vector Meson Production

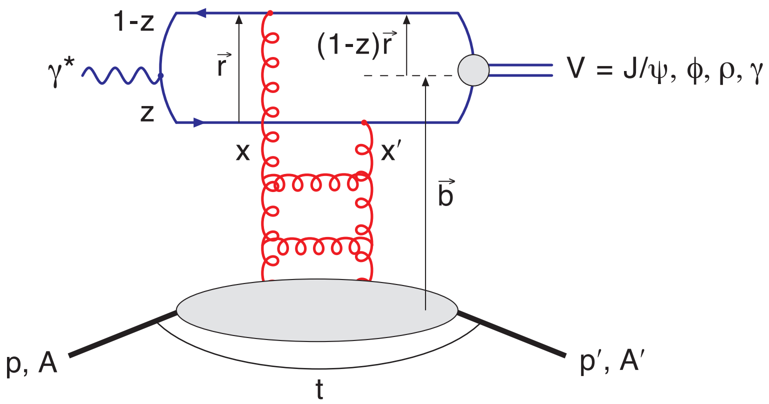

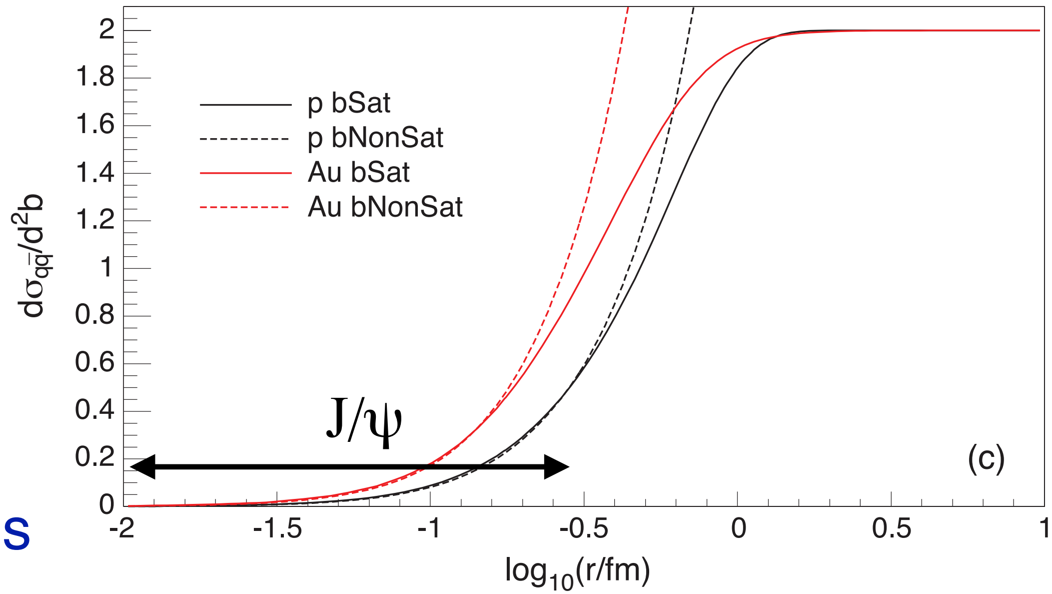

Wave overlap function Ψ*Ψ falls steeply for large dipole radii

- J/ψ not sensitive to saturation.
- Need to look at ϕ, or ρ that "see" more of the dipole amplitude

$$\mathcal{A}^{\gamma^* p \to Vp}_{T,L}(x, Q, \Delta) = i \int \mathrm{d}r \int \frac{\mathrm{d}z}{4\pi} \int \mathrm{d}^2\mathbf{b} (\Psi^*_V \Psi)(r, z) \times 2\pi r J_0([1-z] r \Delta) e^{-i\mathbf{b}\cdot\Delta} \frac{\mathrm{d}\sigma^{(p)}_{q\bar{q}}}{\mathrm{d}^2\mathbf{b}}(x, r, \mathbf{b})$$

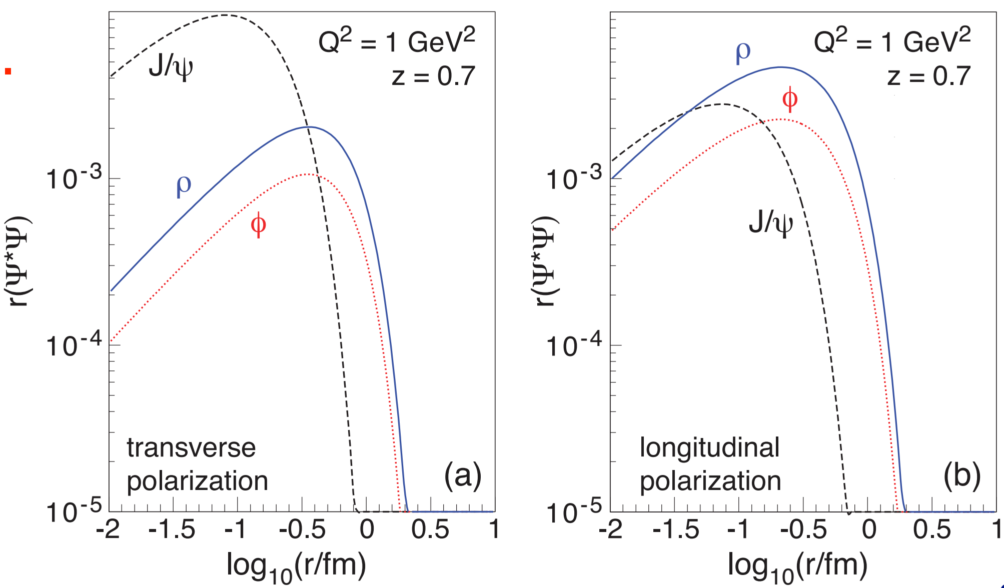

Sartre 1: Diffractive Vector Meson Production

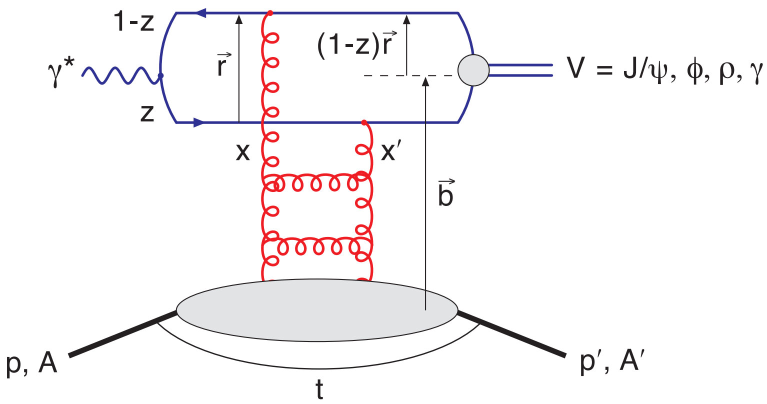

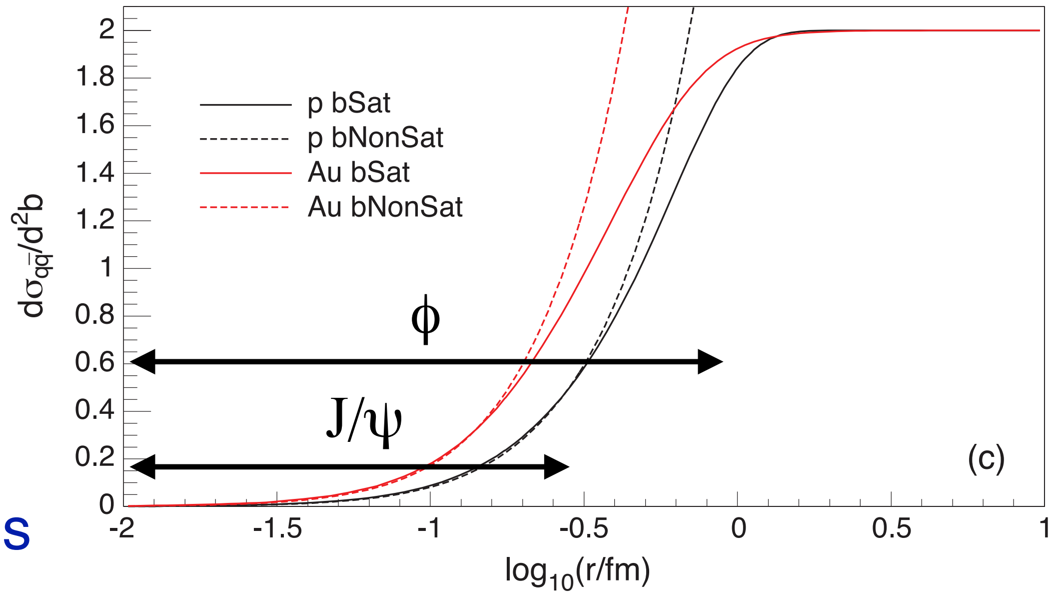

Wave overlap function Ψ*Ψ falls steeply for large dipole radii

- J/ψ not sensitive to saturation.
- Need to look at φ, or ρ that "see" more of the dipole amplitude

$$\mathcal{A}_{T,L}^{\gamma^* p \rightarrow V p}(x, Q, \Delta) = i \int \mathrm{d}r \int \frac{\mathrm{d}z}{4\pi} \int \mathrm{d}^2\mathbf{b} (\Psi_V^* \Psi)(r, z)$$
$$\times 2\pi r J_0([1-z] r \Delta) e^{-i\mathbf{b}\cdot\Delta} \frac{\mathrm{d}\sigma_{q\bar{q}}^{(p)}}{\mathrm{d}^2\mathbf{b}}(x, r, \mathbf{b})$$

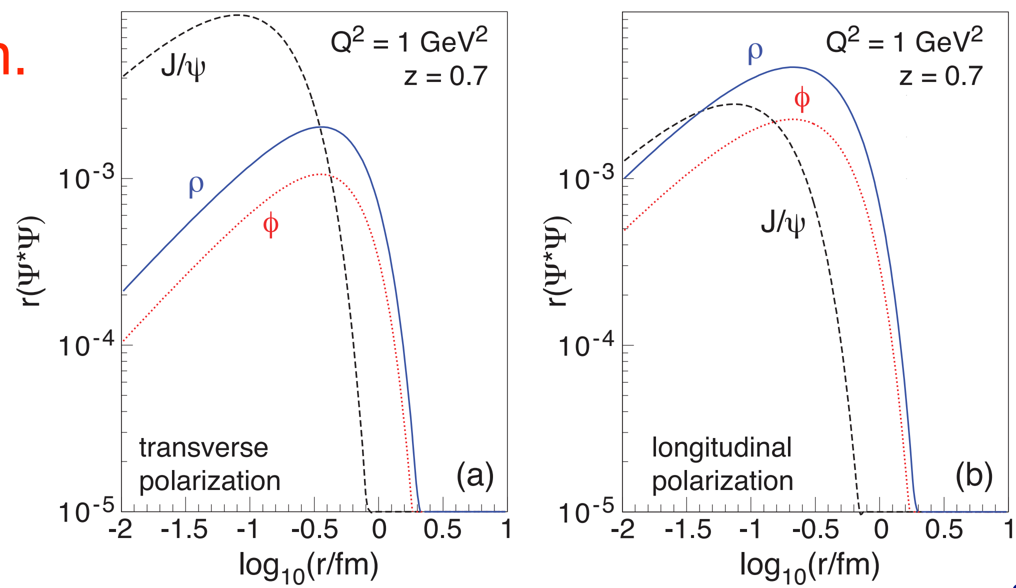

Vector Meson Production: dσ/dt

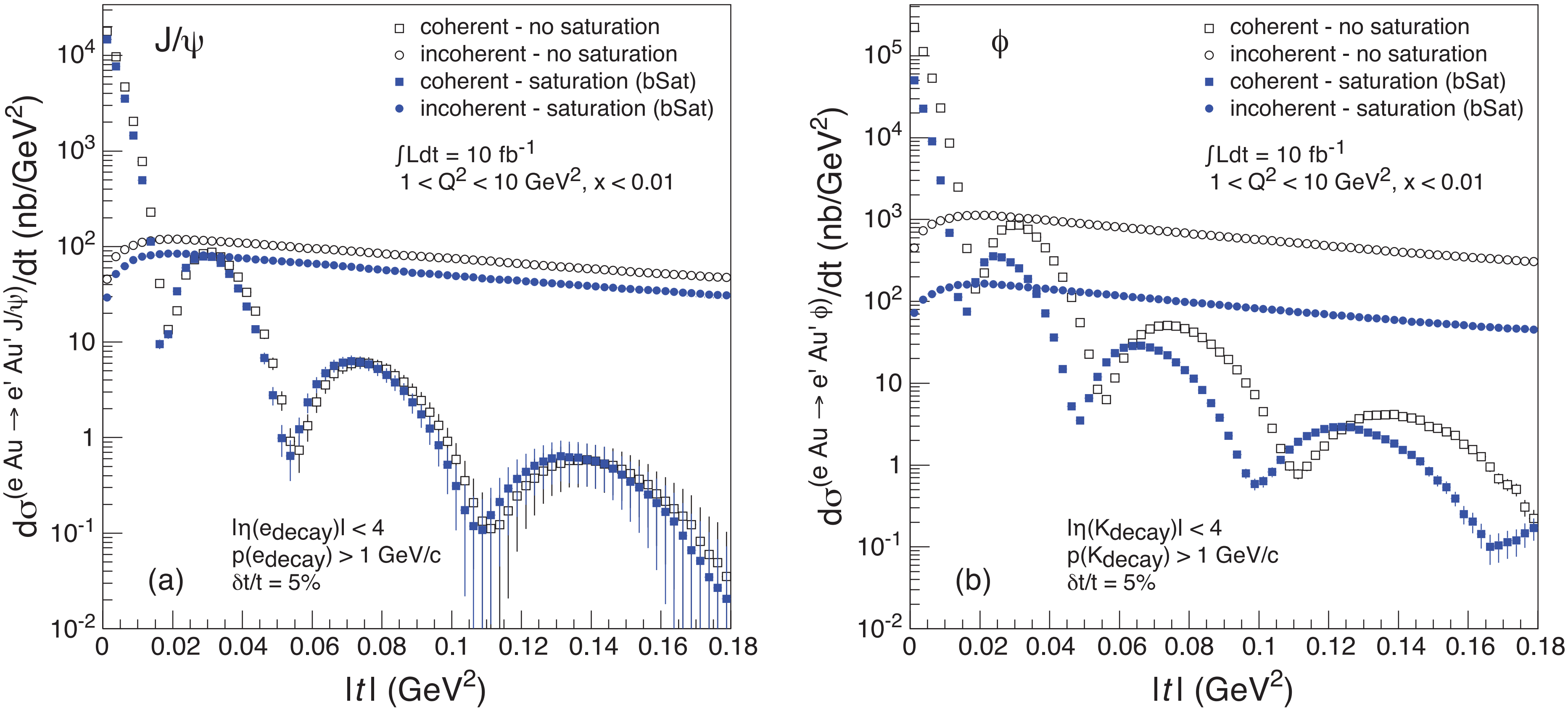

- Find: Typical diffractive pattern for coherent (non-breakup) part
- As expected: J/Ψ less sensitive to saturation than ϕ
- Need this sliced in x bins ⇒ luminosity hungry
- Crucial: t resolution and reach

T. Toll and TU,
PRC 87 (2013) 024913

Spatial Gluon Distribution from $d\sigma/dt$

Diffractive vector meson production: $e + Au \to e' + Au' + J/\psi$

- Momentum transfer $t = |\mathbf{p}_{Au} - \mathbf{p}_{Au'}|^2$ conjugate to b_T

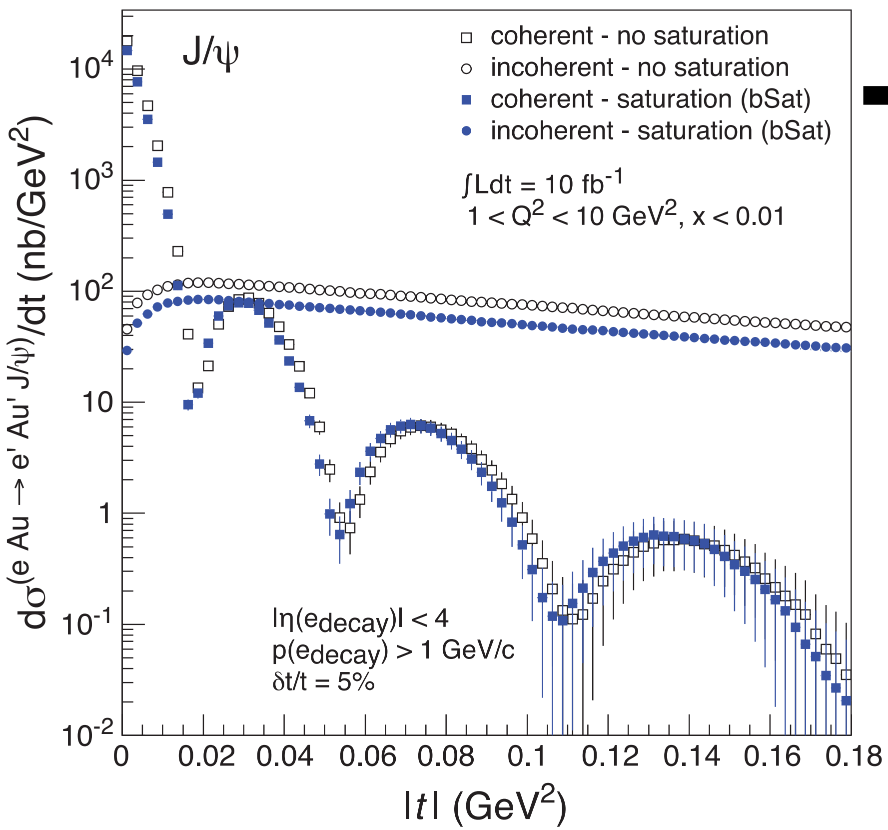

$$F(b) \sim \frac{1}{2\pi} \int_0^\infty d\Delta\, \Delta\, J_0(\Delta b) \sqrt{\frac{d\sigma}{dt}}$$

$t = \Delta^2/(1-x) \approx \Delta^2$

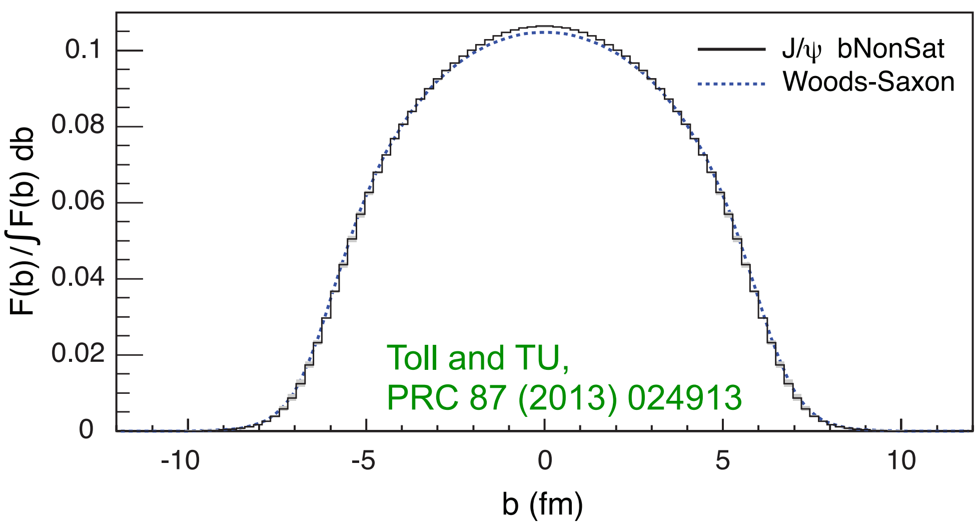

- Converges to input F(b) rapidly: $|t| < 0.1$ almost enough
- Fourier transformation requires $\int$**L**dt **>** 1 fb^{-1}/A

Importance of Incoherent Diffraction

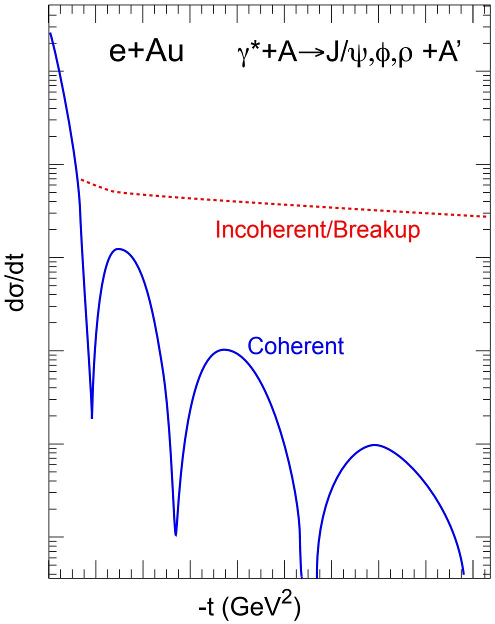

Nucleus dissociates: $f \neq i$

$$\sigma_{\mathrm{incoherent}} \propto \sum_{f \neq i} \langle i|\mathcal{A}|f\rangle \langle f|\mathcal{A}|i\rangle$$

$$= \langle |\mathcal{A}|^2 \rangle - \langle |\mathcal{A}| \rangle^2$$

$$\frac{\mathrm{d}\sigma_{\mathrm{total}}}{\mathrm{d}t} = \frac{1}{16\pi} \langle |\mathcal{A}|^2 \rangle \qquad \frac{\mathrm{d}\sigma_{\mathrm{coherent}}}{\mathrm{d}t} = \frac{1}{16\pi} \langle |\mathcal{A}| \rangle^2$$

Importance of Incoherent Diffraction

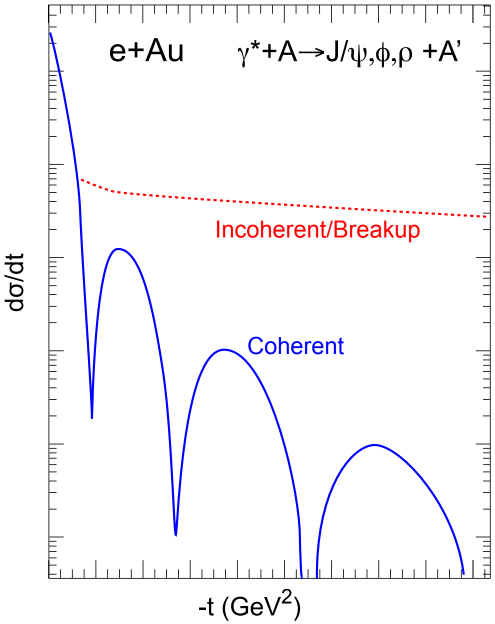

Nucleus dissociates: $f \neq i$

$$\sigma_{\text{incoherent}} \propto \sum_{f \neq i} \langle i|\mathcal{A}|f\rangle \langle f|\mathcal{A}|i\rangle$$

$$= \left\langle |\mathcal{A}|^2 \right\rangle - \left\langle |\mathcal{A}| \right\rangle^2$$

$$\frac{d\sigma_{\text{total}}}{dt} = \frac{1}{16\pi} \left\langle |\mathcal{A}|^2 \right\rangle \qquad \frac{d\sigma_{\text{coherent}}}{dt} = \frac{1}{16\pi} \left\langle |\mathcal{A}| \right\rangle^2$$

- Incoherent CS is the variance of the amplitude ⇒ measure of fluctuation of the source $G(x, Q^2, b)$ at scale ~1/t
- Note: Variance disappears in black disk limit! Clear saturation signature.

Importance of Incoherent Diffraction

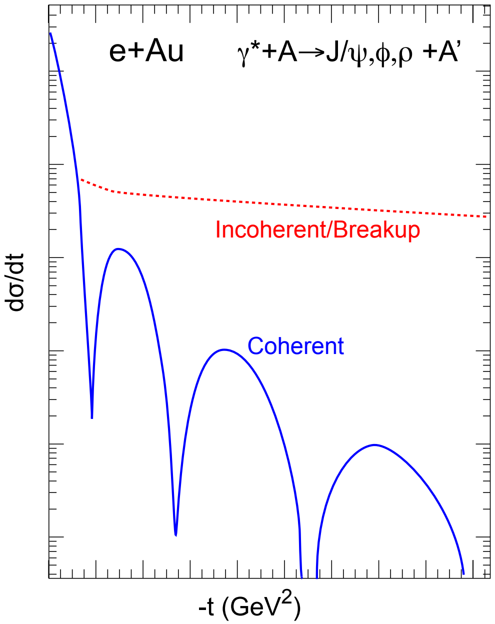

Nucleus dissociates: $f \neq i$

$$\sigma_{\text{incoherent}} \propto \sum_{f \neq i} \langle i|\mathcal{A}|f\rangle \langle f|\mathcal{A}|i\rangle$$

$$= \langle |\mathcal{A}|^2 \rangle - \langle |\mathcal{A}| \rangle^2$$

$$\frac{d\sigma_{\text{total}}}{dt} = \frac{1}{16\pi} \langle |\mathcal{A}|^2 \rangle \qquad \frac{d\sigma_{\text{coherent}}}{dt} = \frac{1}{16\pi} \langle |\mathcal{A}| \rangle^2$$

- Incoherent CS is the variance of the amplitude
  $\Rightarrow$ measure of fluctuation of the source $G(x, Q^2, b)$ at scale ~1/t
- Note: Variance disappears in black disk limit! Clear saturation signature.

Example from ep:

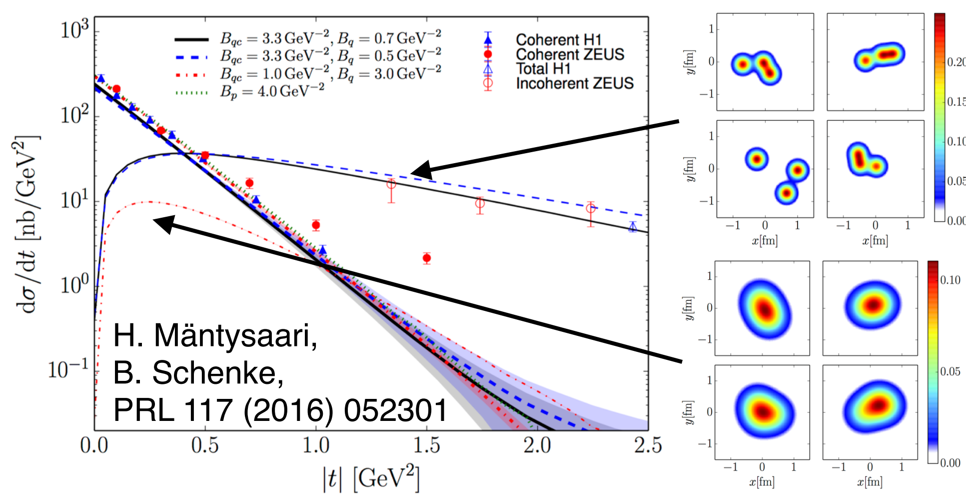

Diffractive over Total Cross-Section

- Saturation models (CGC) predict up to $\sigma_{diff}/\sigma_{tot}$ ~ 25% in eA (Hera in ep ~15%)
- Enhanced at large β, i.e. small M_X^2
  - β = momentum fraction of the struck parton with respect to the Pomeron

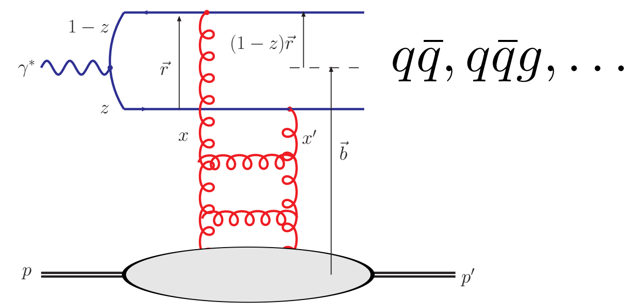

$$\beta \approx \frac{Q^2}{Q^2 + M_X^2} \qquad x = \beta\, x_{I\!P}$$

$$\text{Rapidity Gap} : \approx \ln \beta / x$$

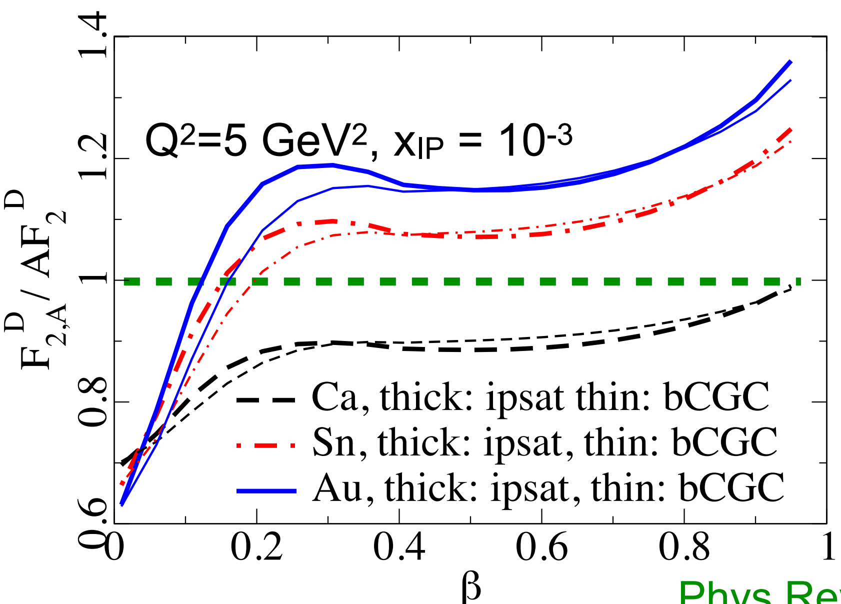

contributions to the proton diffractive structure function

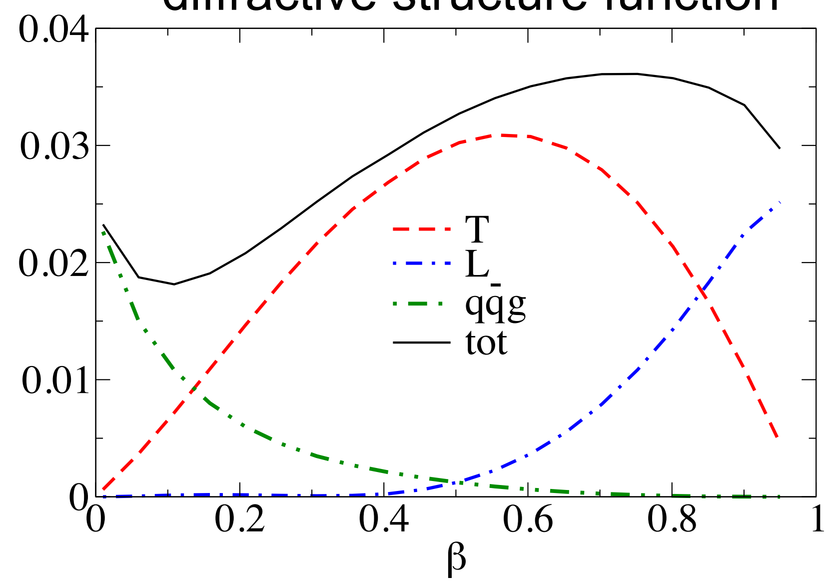

Phys.Rev. C78 (2008) 045201

Key Measurement: $\sigma_{diffractive}/\sigma_{total}$

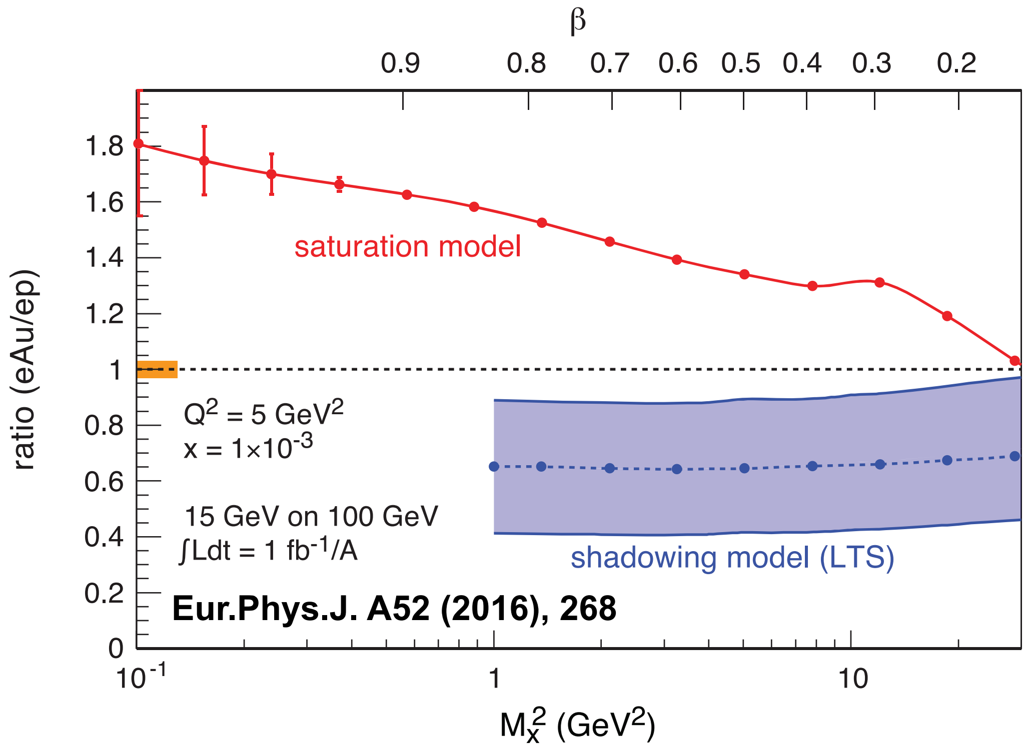

- Studies using diffractive event generator Sartre based on Dipole model.
- Ratio *enhanced* for small M_X and *suppressed* for large M_X
- Standard QCD predicts no M_X dependence and a moderate suppression due to shadowing.

Simple Day 1 Measurement:
Ratio of cross-sections

$$\frac{\sigma_{diff}/\sigma_{total}\ (eA)}{\sigma_{diff}/\sigma_{total}\ (ep)}$$

Unambiguous signature for reaching the saturation limit

Sign Flip

Sign Flip

Sign Change in relative ratio of diffractive structure functions

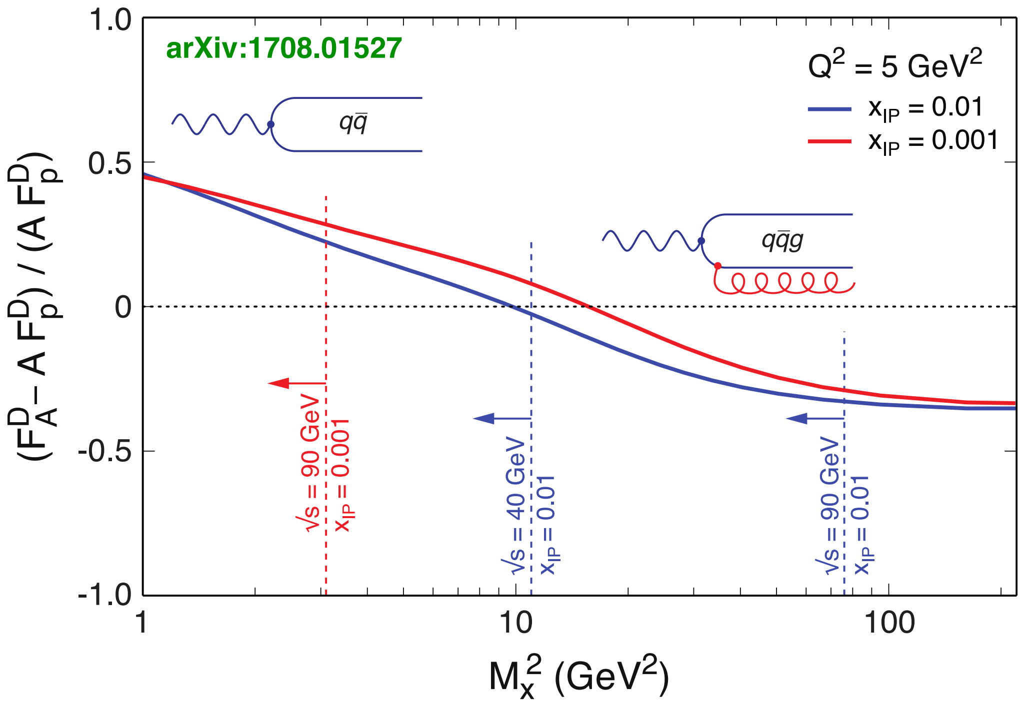

Observing these dependencies on M_x over a wide range in x and Q^2 is crucial!

Nucleus is "blacker" than proton. Elastic scattering probability of a $q\bar{q}$ dipole is maximal in the "black" limit

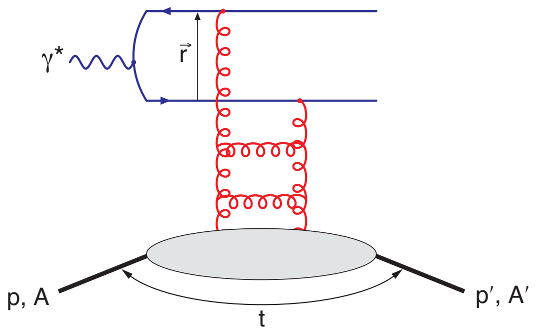

$q\bar{q}g$ component vanishes in black disk limit

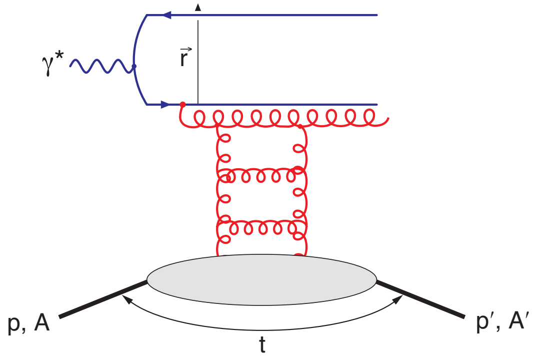

Backup Slides

Exploring Short Range Nuclear Forces

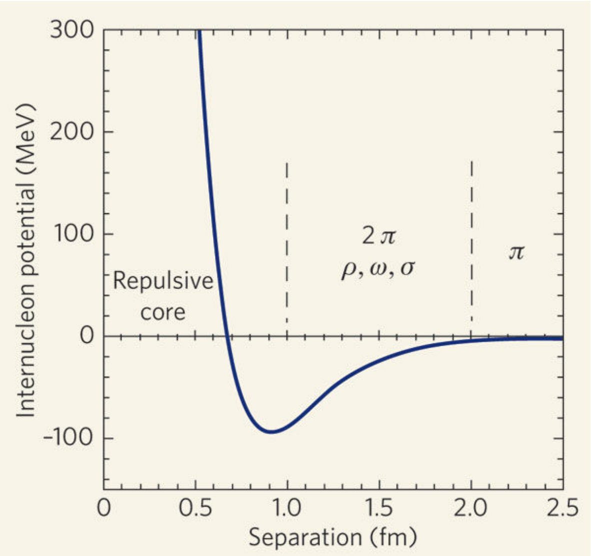

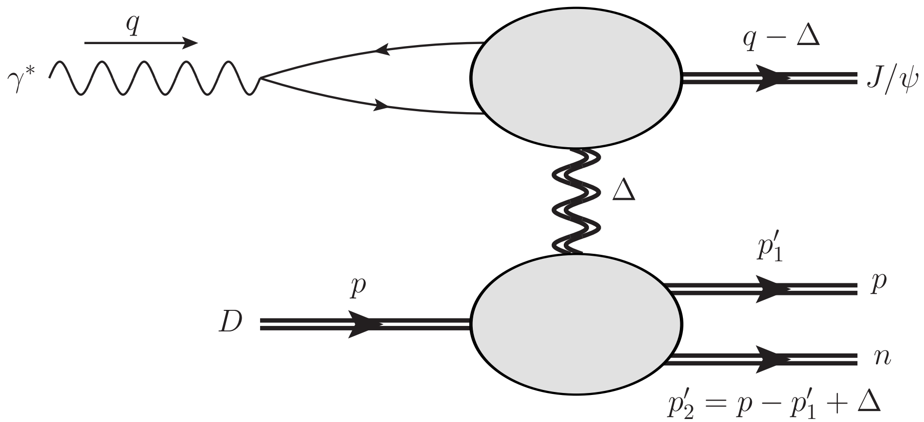

Miller, Sievert, Venugopalan, Phys.Rev. C93 (2016)

- Can the short range contributions to NN scattering be described directly in terms of the quark and gluon DoF in QCD?
- Vector meson production in e+D collisions
  - Cross-section can be expressed in terms of a gluon Transition Generalized Parton Distribution (T-GPD)
  - The hard scale in the final state makes the T-GPD sensitive to the short distance nucleon-nucleon interaction.
- New opportunities - needs more studies (in progress)

Q^2 and A Scaling of Diffractive VM Production

- Saturation models predict very special and strong dependencies in A and Q^2 that are different above and below Q^2_S

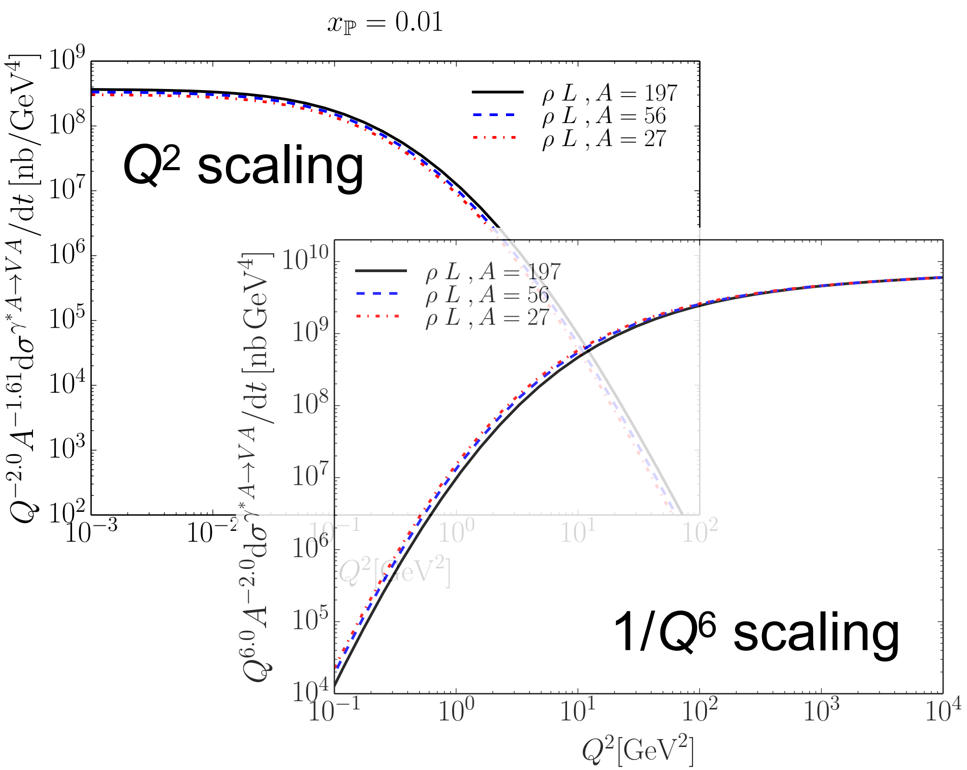

- $Q^2 > Q^2_S$
  - $\sigma \sim 1/Q^6$
  - $\sigma(t=0) \sim A^2$
  - $\sigma \sim A^{4/3}$
- $Q^2 < Q^2_S$
  - $\sigma \sim Q^2$
  - $\sigma(t=0) \sim A^{4/3} \leftrightarrow A^{5/3}$
  - $\sigma \sim A^{2/3} \leftrightarrow A$

- Non-Saturation scenarios do not show this behavior making A, Q^2 dependencies a key measurement

Q^2 and A Scaling of Diffractive VM Production

- Saturation models predict very special and strong dependencies in A and Q^2 that are different above and below Q^2_S

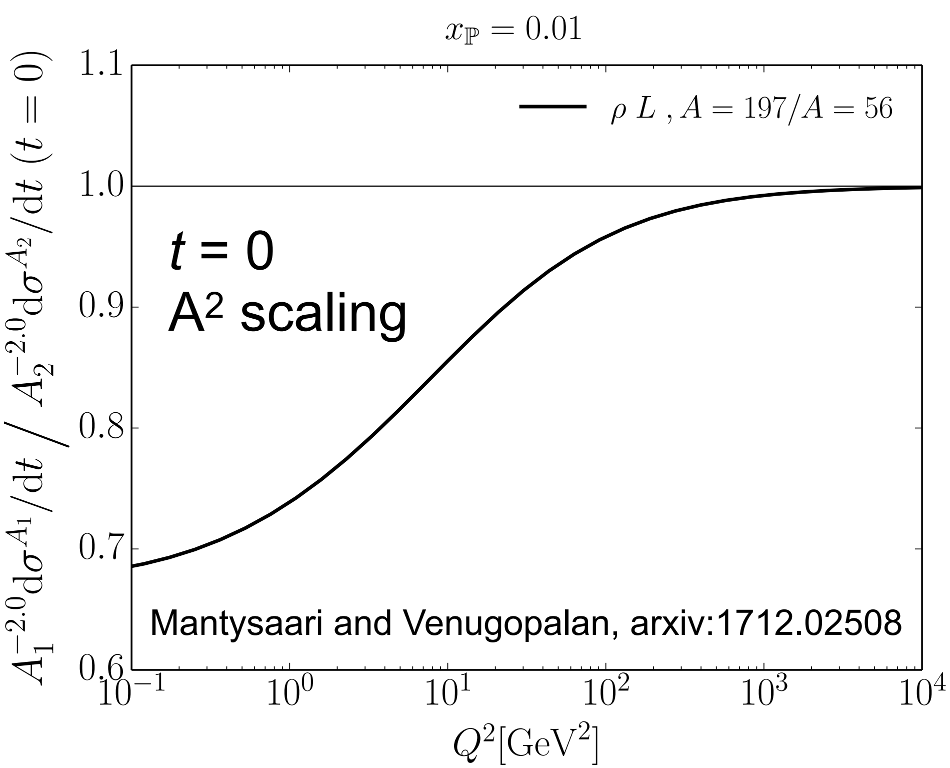

- $Q^2 > Q^2_S$
  - $\sigma \sim 1/Q^6$
  - $\sigma(t=0) \sim A^2$
  - $\sigma \sim A^{4/3}$
- $Q^2 < Q^2_S$
  - $\sigma \sim Q^2$
  - $\sigma(t=0) \sim A^{4/3} \leftrightarrow A^{5/3}$
  - $\sigma \sim A^{2/3} \leftrightarrow A$

- Non-Saturation scenarios do not show this behavior making A, Q^2 dependencies a key measurement

EIC: Gluon TMDs from Dijet Production

- Thus far, focus on quark TMDs while the available studies of gluon TMDs are sparse
- Of particular interest: WW gluon distribution $\mathbf{G^{(1)}}$ and its linearly polarized partner $\mathbf{h_T^{(1)}}$ inside unpolarized hadron
- These gluon distributions play also central role in small-x saturation phenomena.

$G^{(1)}$ and $h_T^{(1)}$ can be accessed through measuring azimuthal anisotropies in processes such as **jet pair (dijet) production** in e+p and e+A scattering.

A. Metz and J. Zhou, Phys. Rev. D84 , 051503 (2011), arXiv:1105.1991.
D. Boer, P. J. Mulders, and C. Pisano, Phys. Rev. D80 , 094017 (2009), arXiv:0909.4652
D. Boer, S. J. Brodsky, P. J. Mulders, and C. Pisano, Phys. Rev. Lett. 106 , 132001 (2011), arXiv:1011.4225.
F. Dominguez, J.-W. Qiu, B.-W. Xiao, and F. Yuan, Phys. Rev. D85 , 045003 (2012), arXiv:1109.6293.
A. Dumitru, L. McLerran, and V. Skokov, Phys. Lett. B743 , 134 (2015), arXiv:1410.4844.
A. Dumitru and V. Skokov, Phys. Rev. D91 , 074006 (2015), arXiv:1411.6630.
A. Dumitru, T. Lappi, and V. Skokov, Phys. Rev. Lett. 115 , 252301 (2015), arXiv:1508.04438.
A. Dumitru and V. Skokov, Phys. Rev. D94 , 014030 (2016), arXiv:1605.02739.

Kinematics: Dijets in γ^*A

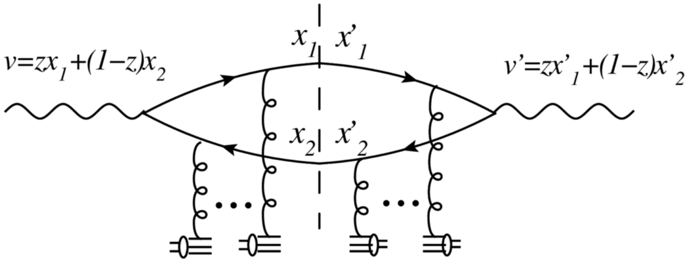

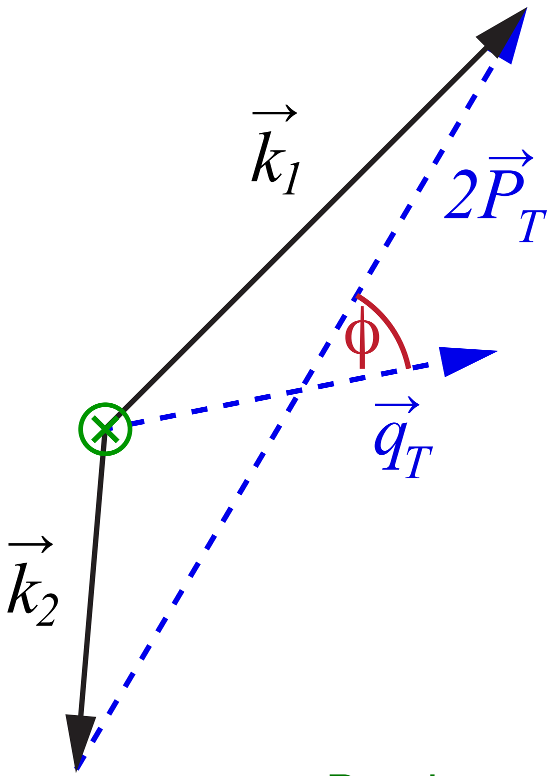

Key observables: P_T and q_T

- the difference in momenta (imbalance)
  $$\vec{q}_T = \vec{k}_1 + \vec{k}_2$$
- the average transverse momentum of the jets
  $$\vec{P}_T = (1-z)\vec{k}_1 - z\vec{k}_2$$
- ϕ is angle between P_T and q_T
- work in "correlation limit" $P_T >> q_T$
- azimuthal asymmetry arising from the linearly polarized gluon distribution: $v_2 = \langle \cos 2\phi \rangle$

Dominguez, Marquet, Xiao, Yuan, PRD 2011

Elliptic Anisotropy in DiJet Production (I)

- Dipartons from McDijet event generator (V. Skokov) → showers via Pythia → experimental cuts → jet-finding with ee-kt (FastJet)

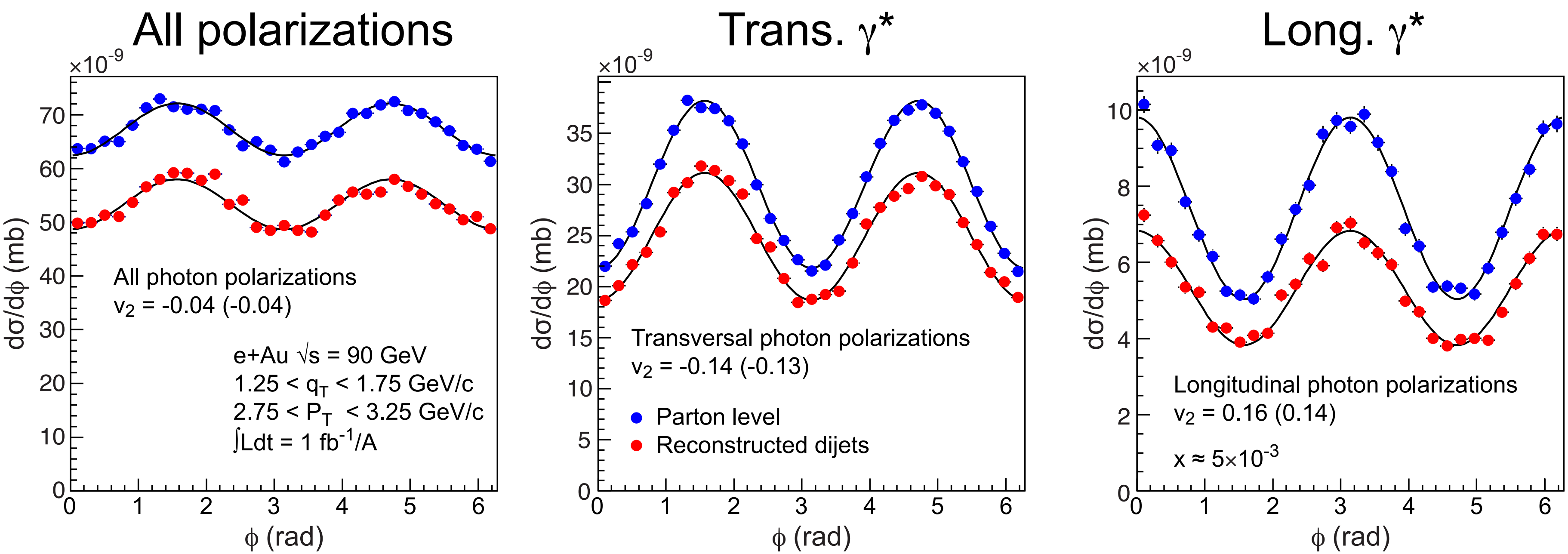

- Dijets recover the anisotropy (v_2) quite well
- NOTE: phase shift between long. and trans. γ^* (dominated by T)

Gluon TMDs via: $$v_2^L = \frac{1}{2}\frac{h_\perp^{(1)}(x,q_\perp)}{G^{(1)}(x,q_\perp)} \quad , \quad v_2^T = -\frac{\epsilon_f^2 P_\perp^2}{\epsilon_f^4 + P_\perp^4}\frac{h_\perp^{(1)}(x,q_\perp)}{G^{(1)}(x,q_\perp)}$$

A. Dumitru, T. Lappi, and V. Skokov, Phys. Rev. Lett. 115 , 252301 (2015), arXiv:1508.04438.

Elliptic Anisotropy in Dijet Production (III)

- Detailed simulations show that in e+A the EIC can perform this challenging measurement
  - Can separate background from signal djets
  - Can separate v_2^L and v_2^T

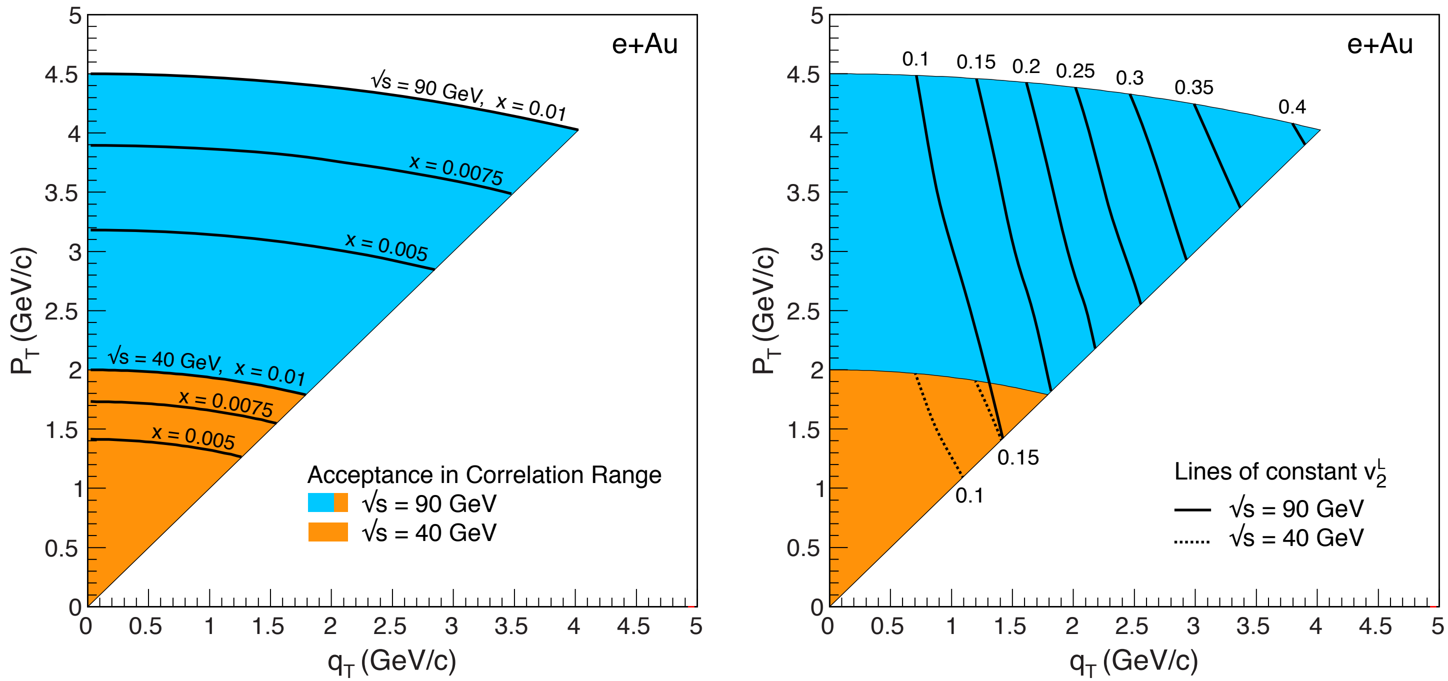

- Measurement requires large EIC energies (jet physics!)

Exclusive Diffractive Vector Meson Production

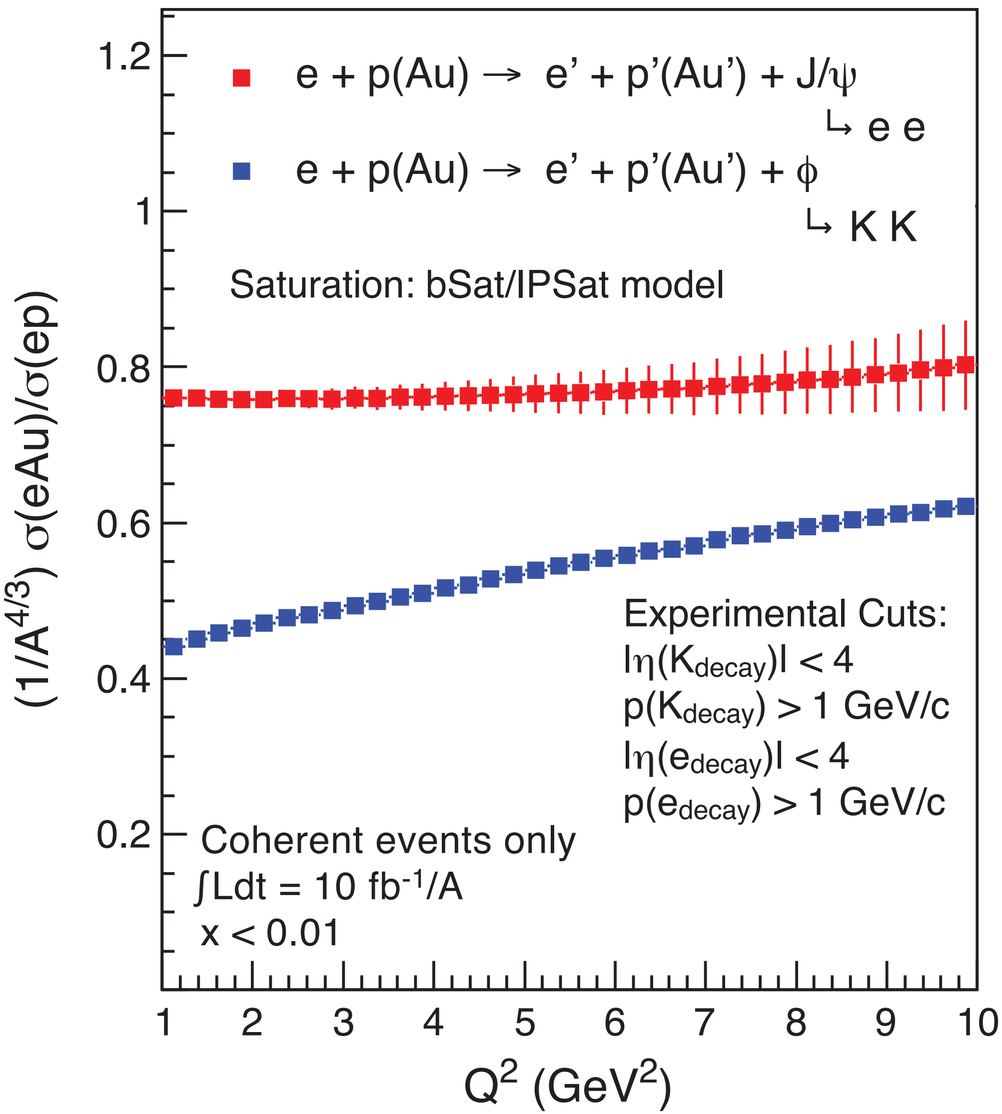

Full simulations using Sartre event generator based on IPSat (aka bSat) model

- Suppression larger for φ than for J/ψ as expected
- Straightforward measurement for early days of an EIC

Note: $A^{4/3}$ scaling strictly only valid at large Q^2

The Problem of Estimating nPDF Constraints

Methods:

- Use σ_{red} (includes F_2 and F_L (F_3)) pseudo data
- Re-weighting EPPS16
  - EPPS16 is a bit stiff at low-x, over-constraints at low-x
- EPPS16* (arXiv:1708.05654, Hannu Paukkunen)
  - more flexible form cures EPPS16 problem (low-x bias)
  - might underestimate impact?

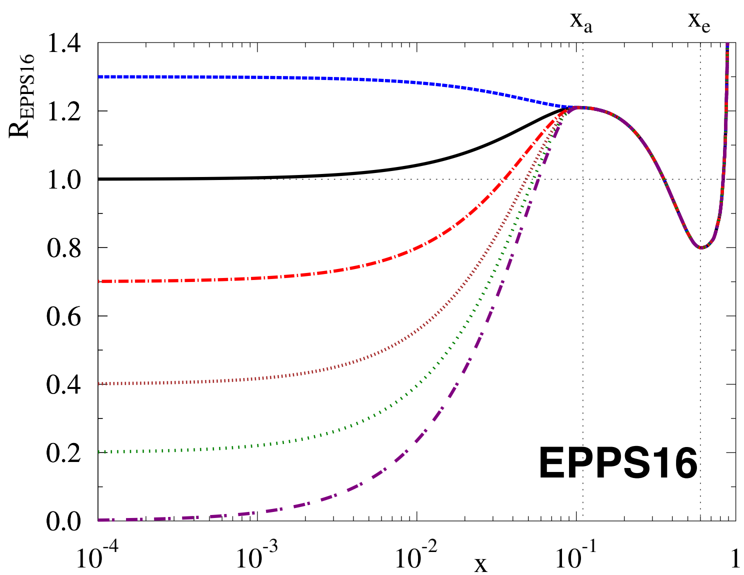

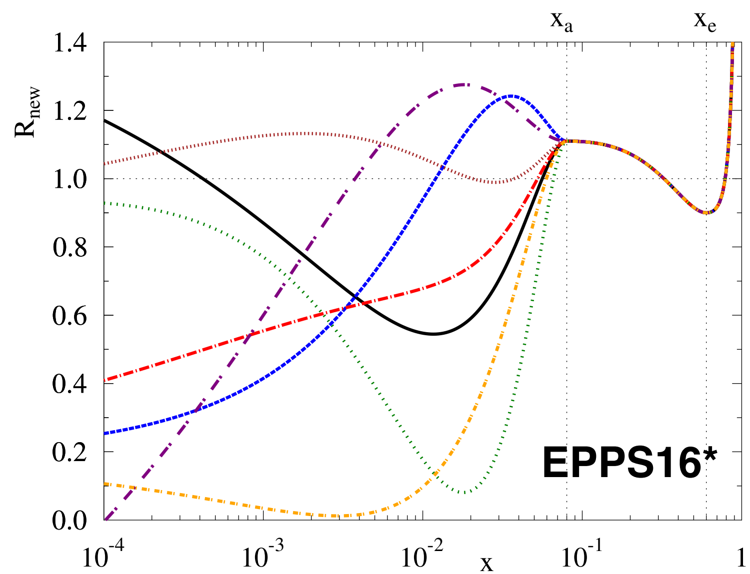

Gluon Saturation: Past Experimental Reach

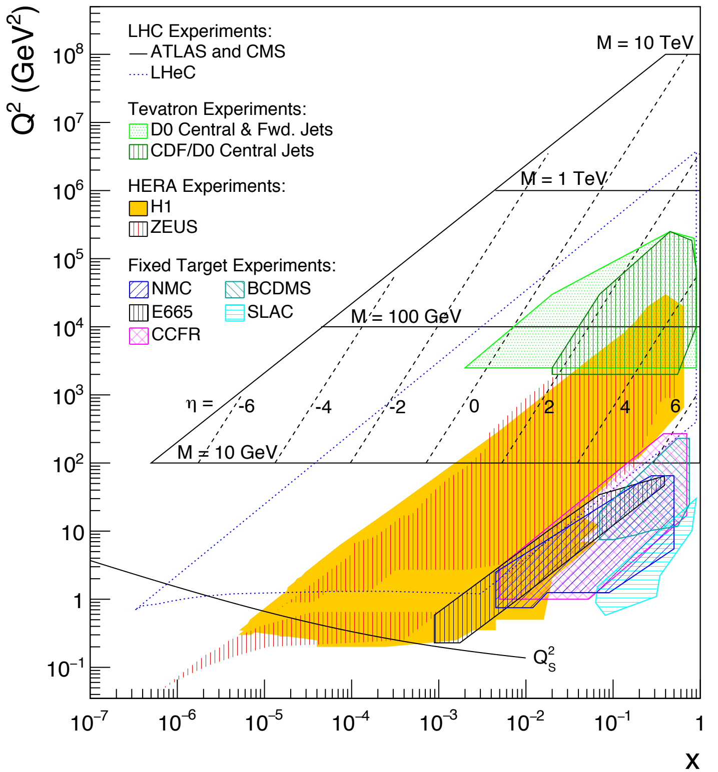

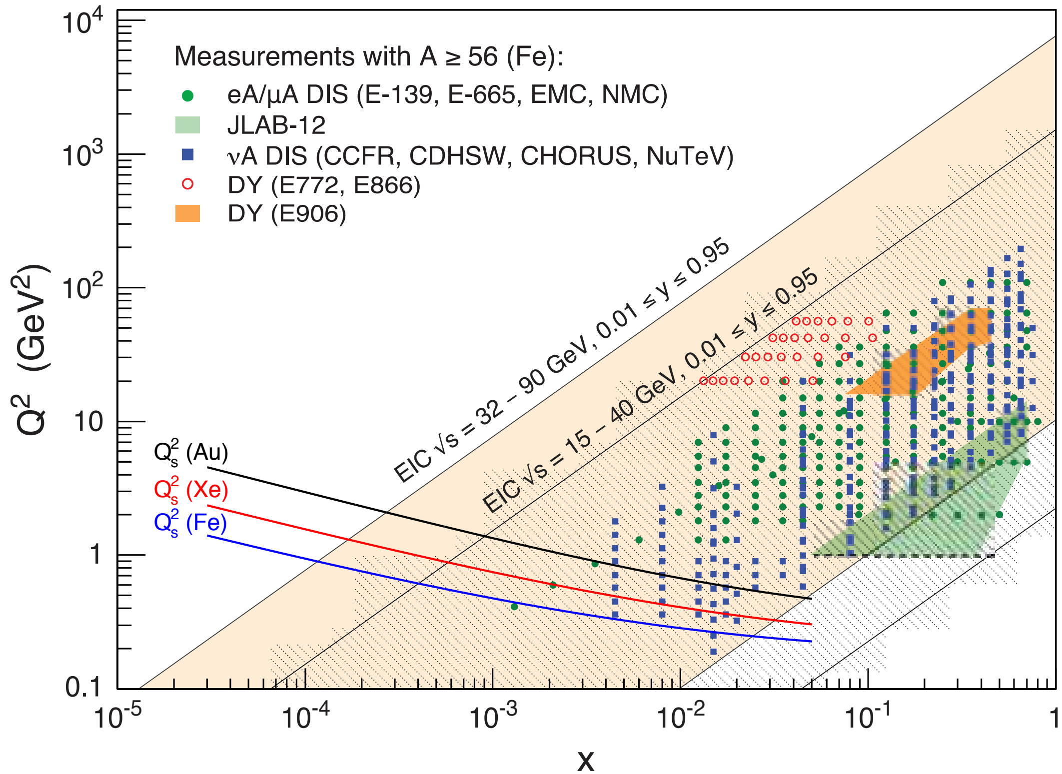

HERA (ep)

- Marginal reach of Q_s
- Only at very low Q^2 making comparison with perturbative QCD impossible

Fixed Target DIS Experiment

- eA, μA, νA
- Same marginal reach
- Only at low Q^2 (Q^2 < 1 GeV^2)

Relation to Chiral Magnetic Effect

- RHIC & LHC: intriguing hints of CME
- Key challenge: understanding dynamics of axial charge production during the very early pre-equilibrium stages (see talk by Niklas Mueller)
- Tuomas Lappi, Soren Schlichting, arXiv:1708.08625
  - Chern-Simons current correlator (the source of axial charge)

$$\langle \dot{\nu}(\mathbf{x})\dot{\nu}(\mathbf{y})\rangle =$$

$$\frac{3g^4 N_\mathrm{c}^2(N_\mathrm{c}^2-1)}{32}\left[\left(G^{(1)}_{(U)}(\mathbf{x},\mathbf{y})\right)^2\left(G^{(1)}_{(V)}(\mathbf{x},\mathbf{y})\right)^2-\left(h^{(1)}_{\perp(U)}(\mathbf{x},\mathbf{y})\right)^2\left(h^{(1)}_{\perp(V)}(\mathbf{x},\mathbf{y})\right)^2\right]$$

Immediate link between dijet DIS (and TMDs) and CME